

SLIDE: a surrogate fairness constraint to ensure fairness consistency

Kunwoong Kim^a, Ilsang Ohn^b, Sara Kim^{c,*}, Yongdai Kim^{a,d,**}

^a*Department of Statistics, Seoul National University, Seoul, 08826, Republic of Korea*

^b*Department of Applied and Computational Mathematics and Statistics, University of Notre Dame, State of Indiana, 46556, United States of America*

^c*Core Technology R&D team, Mechatronic R&D Center, Samsung Electronics, Hwaseong, 18448, Republic of Korea*

^d*School of Data Science, Seoul National University, Seoul, 08826, Republic of Korea*

Abstract

As they have a vital effect on social decision makings, AI algorithms should be not only accurate and but also fair. Among various algorithms for fairness AI, learning a prediction model by minimizing the empirical risk (e.g., cross-entropy) subject to a given fairness constraint has received much attention. To avoid computational difficulty, however, a given fairness constraint is replaced by a surrogate fairness constraint as the 0-1 loss is replaced by a convex surrogate loss for classification problems. In this paper, we investigate the validity of existing surrogate fairness constraints and propose a new surrogate fairness constraint called SLIDE, which is computationally feasible and asymptotically valid in the sense that the learned model satisfies the fairness constraint asymptotically and achieves a fast convergence rate. Numerical experiments confirm that the SLIDE works well for various benchmark datasets.

Keywords: Fairness AI, learning theory

*This work was done when the author was affiliated with Department of Statistics, Seoul National University, Seoul, 08826, Republic of Korea.

**Corresponding author

Email addresses: kwkim.online@gmail.com (Kunwoong Kim), iohn@nd.edu (Ilsang Ohn), kimsarah@snu.ac.kr (Sara Kim), ydkim0903@gmail.com (Yongdai Kim)

1. Introduction

Recently, AI (Artificial Intelligence) is being used as decision making tools in various domains such as credit scoring, criminal risk assessment, education of college admissions [1]. As AI has a wide range of influences on human social life, issues of transparency and ethics of AI are emerging. However, it is widely known that due to the existence of historical bias in data against ethics or regulatory frameworks for fairness, trained AI models based on such biased data could also impose bias or unfairness against a certain sensitive group (e.g., non-white, women) [2, 3]. Therefore, designing an AI algorithm that is accurate and fair simultaneously has become a crucial research topic.

The two important issues in fairness AI are definitions of fairness and algorithms to learn fair prediction models. There are various definitions of fairness AI, which are roughly categorized into two groups - *group fairness* and *individual fairness*. Group fairness [4, 5, 6] focuses on treating fairly each sensitive group while individual fairness [7] focuses on treating fairly any similar individuals.

Once the definition of fairness is selected, the next step for fairness AI is to choose a learning algorithm to find a fair classifier that is not only accurate but also fair. Most fair learning algorithms belong to one of the three categories - pre-processing, in-processing and post-processing methods. Pre-processing methods remove bias in training dataset or find a fair representation with respect to sensitive variables before the training phase and learn AI models based on de-biased data or fair representations [8, 9, 10, 11, 12, 13, 14, 15, 16]. In-processing methods generally train an AI model by minimizing the cost function subject to a given fairness constraint [17, 18, 19, 20, 21, 22, 23, 24, 25, 26, 27, 28].

Post-processing methods first learn an AI model without any fairness constraint and then transform the decision boundary or score function of the trained AI model for each sensitive group to satisfy a given fairness constraint [29, 30, 6, 31, 32, 33, 34, 35].

In this paper, we are concerned with in-processing fairness AI algorithms. A difficulty in in-processing algorithms is that most fairness constraints involve the indicator function $\mathbb{I}(\cdot > 0)$ which makes the optimization infeasible. To resolve this problem, a popular approach is to replace $\mathbb{I}(\cdot > 0)$ by a computationally easier surrogate function such as the hinge function $(1 + \cdot)_+$. This hinge function is the tight convex upper bound of the indicator function and hence popularly used for a surrogate loss function of the 0-1 loss. Moreover, it is known that the hinge loss is Fisher-consistent in the sense that the minimizer of the population risk with respect to the hinge loss is equal to the Bayes risk [36, 37, 38]. Thus, we can estimate the Bayes classifier consistently by minimizing the empirical risk with respect to the hinge loss under regularity conditions.

The question we address in this paper is whether this nice property of the hinge function as a surrogate loss of the 0-1 loss is still valid for the fairness constraint. That is, we investigate whether in-processing learning algorithms with a surrogate fairness constraint yield prediction models which are (asymptotically) fair in terms of the original fairness constraint. Asymptotic properties of fairness AI algorithms have been studied by [39, 40]. [39] proposed a two-step procedure to find a prediction model which is asymptotically fair. However, as noted by the authors, the proposed algorithm is not computationally feasible since it involves indicator functions in the objective function to be minimized. [40] and [18, 41, 34] showed that the linear- and the hinge-surrogate fairness constraints are not much different from the original fairness constraint. However, no result about an asymptotic guarantee of fairness has been obtained. In addition, [42] raised an issue that using such surrogate fairness constraints cannot guarantee a given fairness constraint due to the gap between the original constrained function space and the surrogate one. Our empirical studies illustrate that the hinge-surrogate fairness constraint does not provide the optimal model under the original fairness constraint. See Figure 2 for illustration.

The aim of this research is to propose a new surrogate fairness constraint that makes the optimization feasible and provides the optimal prediction model under the original fairness constraint asymptotically. For this purpose, we de-

velop a new surrogate function called SLIDE for the indicator function. We prove that the minimizer of the empirical risk subject to the SLIDE-surrogate fairness constraint is asymptotically equivalent to the minimizer of the population risk under the original fairness constraint.

Our contributions are summarized as follows.

- We propose a new surrogate fairness constraint called SLIDE, which is computationally feasible and has desirable theoretical properties.
- We prove that the SLIDE is an asymptotically valid surrogate fairness constraint by deriving the fairness convergence rate as well as the risk convergence rate of prediction models trained by in-processing methods with the SLIDE-surrogate fairness constraint.
- We empirically demonstrate by analyzing several benchmark datasets that the SLIDE-surrogate fairness constraints are superior to the hinge-surrogate fairness constraints.

2. Learning algorithms for fairness AI: Review

Let (Y, \mathbf{X}, Z) be the random vector of a triplet of output, input and sensitive variables, whose distribution is P . For simplicity, we consider a binary classification problem (i.e. $Y \in \{-1, 1\}$) and a binary sensitive variable (i.e. $Z \in \{0, 1\}$). For a given loss function l and a class of prediction models \mathcal{F} , the aim of supervised learning is to find f^* defined as $f^* = \operatorname{argmin}_{f \in \mathcal{F}} \mathbf{E}\{l(Y, f(\mathbf{X}))\}$. Due to historical biases or social prejudices, the optimal prediction model f^* would not be socially acceptable because it treats certain groups or individuals unfairly. Thus, we want to search f which is fair and at the same time makes the population risk $\mathbf{E}\{l(Y, f(\mathbf{X}))\}$ as small as possible.

Suppose that $\mathcal{F}_{\text{fair}}$ is a subset of \mathcal{F} which consists of all fair prediction models. Then, the goal of fair supervised learning is to find f_{fair}^* defined as $f_{\text{fair}}^* = \operatorname{argmin}_{f \in \mathcal{F}_{\text{fair}}} \mathbf{E}\{l(Y, f(\mathbf{X}))\}$. There exist numerous definitions for the fairness

model class $\mathcal{F}_{\text{fair}}$, most of which can be formulated as

$$\mathcal{F}_{\text{fair}} = \{f \in \mathcal{F} : \phi(f) \leq \alpha\}$$

for a positive constant α , where $\phi : \mathcal{F} \rightarrow [0, \infty)$ is a so called *fairness constraint* function corresponding to a given definition of fairness. In the next subsection, two representative fairness constraints are explained, which we focus for theoretical derivations and empirical studies. Our theoretical results, however, can be applied to most of other fairness constraints without much modification.

2.1. Examples of fairness constraints

We consider two representative fairness constraints - one for group fairness and the other for individual fairness. For a given real-valued function f and an input \mathbf{X} , the corresponding classifier is constructed by $\text{sign}\{f(\mathbf{X})\}$.

Disparate Impact: The first fairness constraint is disparate impact (DI) [5]. A prediction model f satisfies the α -DI if $\phi(f) \leq \alpha$, where

$$\phi(f) = |\mathbf{P}(f(\mathbf{X}) \geq 0 | Z = 0) - \mathbf{P}(f(\mathbf{X}) \geq 0 | Z = 1)|. \quad (1)$$

Other group fairness constraints can be defined by replacing $\mathbf{P}(f(\mathbf{X}) \geq 0 | Z = z)$ in (1) for $z \in \{0, 1\}$ by other conditional probabilities. For example, the equalized odds (EO) and equal opportunity (EqOpp) [6] are defined by replacing $\mathbf{P}(f(\mathbf{X}) \geq 0 | Z = z)$ into $\mathbf{P}(f(\mathbf{X}) \geq 0 | Z = z, Y = y)$ for $y \in \{-1, 1\}$ and $\mathbf{P}(f(\mathbf{X}) \geq 0 | Z = z, Y = 1)$ respectively.

Uniform Individual fairness: Individual fairness requires that similar individuals should be treated similarly. [7] introduces the initial notion of individual fairness: we say a classifier $f \in \mathcal{F}$ is individually fair if it satisfies the Lipschitz property, i.e., for every $\mathbf{x}, \mathbf{x}' \in \mathcal{X}$, $D(f(\mathbf{x}), f(\mathbf{x}')) \leq d(\mathbf{x}, \mathbf{x}')$ with respect to a similarity metric $D(\cdot, \cdot)$ between prediction models and a similarity metric $d(\cdot, \cdot)$ between individuals. [43] introduces a relaxed notion: a classifier $f \in \mathcal{F}$ is (α, γ) -approximately individually fair if it satisfies $\mathbf{P}_{\mathbf{x}, \mathbf{x}'}\{D(f(\mathbf{x}), f(\mathbf{x}')) - d(\mathbf{x}, \mathbf{x}') > \gamma\} \leq \alpha$ for a given $\gamma > 0$. In this paper, we consider a new definition of individual fairness called $(\alpha, \gamma, \epsilon)$ -uniform individual fair (UIF) defined

as $\phi(f; \gamma, \epsilon) \leq \alpha$, where

$$\phi(f; \gamma, \epsilon) := \mathbf{P}(\sup_{\mathbf{v}: d(\mathbf{X}, \mathbf{v}) \leq \epsilon} D(f(\mathbf{X}), f(\mathbf{v})) > \gamma). \quad (2)$$

The definition of UIF is motivated by the definition of SenSeI [44] which requires that

$$\mathbf{E}(\sup_{\mathbf{v}: d(\mathbf{X}, \mathbf{v}) \leq \epsilon} D(f(\mathbf{X}), f(\mathbf{v}))) \leq \alpha.$$

We replace the expectation by the probability even though one more parameter (i.e. γ) is needed. In the section of experiments, we show that UIF is better than SenSeI.

2.2. Learning algorithms for fairness AI

Let $(y_1, \mathbf{x}_1, z_1), \dots, (y_n, \mathbf{x}_n, z_n)$ be given training dataset which are assumed to be independent realizations of (Y, \mathbf{X}, Z) . Let ϕ_n be the empirical version of ϕ . The ϕ_n for DI and UIF are given as

$$\phi_n(f) = \left| \frac{1}{n_0} \sum_{i: z_i=0} \mathbb{I}(f(\mathbf{x}_i) > 0) - \frac{1}{n_1} \sum_{i: z_i=1} \mathbb{I}(f(\mathbf{x}_i) > 0) \right| \quad (3)$$

and

$$\phi_n(f; \gamma, \epsilon) = \frac{1}{n} \sum_{i=1}^n \mathbb{I}(D(f(\mathbf{x}_i), f(\mathbf{v}'_i)) > \gamma) \quad (4)$$

respectively, where $n_z = \sum_{i=1}^n \mathbb{I}(z_i = z)$ and $\mathbf{v}'_i = \arg \max_{\mathbf{v}: d(\mathbf{x}_i, \mathbf{v}) \leq \epsilon} D(f(\mathbf{x}_i), f(\mathbf{v}))$.

Let $\mathcal{F}_{n,\alpha} = \{f \in \mathcal{F} : \phi_n(f) \leq \alpha\}$. Most in-processing fair learning algorithms try to minimize the empirical risk $L_n(f)$ on $\mathcal{F}_{n,\alpha}$, where $L_n(f) = \sum_{i=1}^n l(y_i, f(\mathbf{x}_i))/n$. However, this optimization is hard since ϕ_n is not continuous. Typically this problem is resolved by use of a surrogate fairness constraint. One of the most popular surrogate fairness constraint is to replace the indicator function $\mathbb{I}(\cdot \geq 0)$ in ϕ_n by the hinge function $(1 + \cdot)_+$, which we denote $\phi_n^{\text{hinge}}(f)$ and $\phi_n^{\text{hinge}}(f; \gamma, \epsilon)$. Then, we learn a prediction model by minimizing the empirical risk subject to $\phi_n^{\text{hinge}}(f) \leq \alpha$ which is similar to [18, 40, 41, 34].

3. SLIDE: A new surrogate fairness constraint

For a fixed $\alpha > 0$ and any $\delta > 0$, we say that a trained prediction model \hat{f}_n is fairness-consistent if $\mathbf{P}\{\phi(\hat{f}_n) \leq \alpha + \delta\} \rightarrow 1$ as $n \rightarrow \infty$. The aim of this section is to propose a new surrogate fairness constraint with which the corresponding (in-process) trained prediction model is fairness-consistent.

The hinge function is popularly used as a surrogate loss function of the 0-1 loss in classification problems, and it is shown that the resulting estimator is risk-consistent in the sense that the mis-classification error of the trained prediction models converges to that of the Bayes classifier [36, 37, 38]. This nice property of the hinge function, however, would not hold for fairness-consistency. This is mainly because the surrogate fairness constraint may not be asymptotically equivalent to the original fairness constraint. To resolve this problem, we propose a new surrogate function so-called SLIDE for the indicator function $\mathbb{I}(\cdot > 0)$ such that the corresponding surrogate fairness constraint is asymptotically equivalent to the original fairness constraint, and thus the resulting prediction model becomes fairness-consistent as well as risk-consistent.

3.1. Proposed surrogate fairness constraint: SLIDE

For a given $\tau > 0$, the SLIDE function $\nu_\tau(\cdot) : \mathbb{R} \rightarrow [0, 1]$ is defined as

$$\nu_\tau(z) = \frac{z}{\tau} \mathbb{I}(0 < z \leq \tau) + \mathbb{I}(z > \tau). \quad (5)$$

Figure 1 compares the 0-1, the hinge and SLIDE functions. The function ν_τ looks similar to a slide so that we call it SLIDE. Note that the SLIDE function is a lower bound of the 0-1 function while the hinge function is an upper bound. In addition, the SLIDE function is non-convex while the hinge function is convex. The non-convexity would make the corresponding optimization more difficult, but our experiments suggest that standard gradient descent based optimization algorithms work well with the SLIDE function. Moreover, it is possible to apply convex-concave procedure (CCCP) of [45] since $\nu_\tau(\cdot)$ is decomposed by the sum of convex and concave functions. See section of experiments for

details. The empirical SLIDE-surrogate fairness constraints for DI and UIF are obtained by replacing $\mathbb{I}(\cdot > 0)$ in ϕ_n by $\nu_\tau(\cdot)$, which we denote $\phi_{n,\tau}^{\text{slide}}(f)$ and $\phi_{n,\tau}^{\text{slide}}(f; \gamma, \epsilon)$, respectively. We also denote $\phi_\tau^{\text{slide}}(f)$ and $\phi_\tau^{\text{slide}}(f; \gamma, \epsilon)$ as population version of both, respectively. For notational simplicity, we omit the superscript “slide” when the meaning is clear.

The SLIDE function is motivated by the Ψ learning of [46], where $\Psi(z) = (z/\tau) \cdot \mathbb{I}(-\tau < z \leq 0) + \mathbb{I}(z > 0)$ is used as a surrogate loss of the negative 0-1 loss. Even though the Ψ function is an upper bound of the indicator function, it would not be appropriate for a surrogate fairness constraint since $\phi_n(f)$ depends on samples with $-\tau < f(\mathbf{x}_i) < 0$ for some $i \in \{1, \dots, n\}$. We modify the Ψ function to have the SLIDE function.

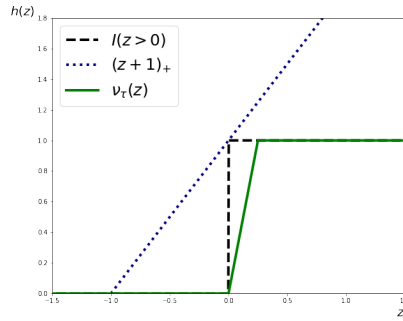


Figure 1: Comparison of the 0-1, hinge and the SLIDE ($\tau = 0.25$) functions (black long dotted line: 0-1, blue short dotted line: hinge, and green solid line: the SLIDE).

3.2. Comparison of the SLIDE- and the hinge-surrogate fairness constraints with a toy example

Let $\mathcal{F}_{n,\alpha}^{\text{hinge}} = \{f \in \mathcal{F} : \phi_n^{\text{hinge}}(f) \leq \alpha\}$ and $\mathcal{F}_{n,\alpha,\tau}^{\text{slide}} = \{f \in \mathcal{F} : \phi_{n,\tau}^{\text{slide}}(f) \leq \alpha\}$. In this section, by analyzing a toy example, we illustrate that $\mathcal{F}_{n,\alpha,\tau}^{\text{slide}}$ is closer to the original constraint class $\mathcal{F}_{n,\alpha}$ than $\mathcal{F}_{n,\alpha}^{\text{hinge}}$ is.

The left panel of Figure 2 presents the toy dataset with two dimensional samples which are generated from a mixture of two Gaussian distributions whose details are given in Appendix. We consider linear model as $\mathcal{F} = \{f_\beta(\mathbf{x}) = \beta_1 x_1 + \beta_2 x_2 : \beta := (\beta_1, \beta_2)^\top \in (-1, 1)^2\}$. For the fairness constraint, we consider

the relaxed individual fairness in [43] as $\phi_{\text{if}}(f; \gamma) = \mathbf{P}_{\mathbf{X}, \mathbf{X}'} \{D(f(\mathbf{X}), f(\mathbf{X}')) - d(\mathbf{X}, \mathbf{X}') > \gamma\}$ with $\gamma = 0.3$, where \mathbf{X}' is an independent copy of \mathbf{X} .

We calculate $\mathcal{F}_{n,\alpha}$, $\mathcal{F}_{n,\alpha}^{\text{hinge}}$ and $\mathcal{F}_{n,\alpha,\tau}^{\text{slide}}$ by grid search and compare them as follows. Let $\Theta_{n,\alpha} = \{\beta : f_\beta \in \mathcal{F}_{n,\alpha}\}$, and $\Theta_{n,\alpha}^{\text{hinge}}$ and $\Theta_{n,\alpha,\tau}^{\text{slide}}$ are defined accordingly. We obtain those sets of fair parameters by calculating the population version of the fairness constraint values (i.e., $\phi_{\text{if}}(f; \gamma)$) based on Monte-Carlo simulation at the gridly selected parameters (i.e., (β_1, β_2)) on the 200×200 grids of $(-1, 1) \times (-1, 1)$.

Let $D_H(\cdot, \cdot)$ be the Hausdorff distance between two subsets in $(-1, 1)^2$. It turns out that

$$D_H(\Theta, \Theta') = \max \{D_{H,1}, D_{H,2}\}$$

where $D_{H,1} := \sup_{\theta \in \Theta} \inf_{\theta' \in \Theta'} \|\theta - \theta'\|_2$ and $D_{H,2} := \sup_{\theta' \in \Theta'} \inf_{\theta \in \Theta} \|\theta - \theta'\|_2$ for two subsets Θ and Θ' . We calculate $d_\alpha^{\text{hinge}} = \min_{\alpha'} D_H(\Theta_{n,\alpha}, \Theta_{n,\alpha'}^{\text{hinge}})$ and $d_{\alpha,\tau}^{\text{slide}} = \min_{\alpha'} D_H(\Theta_{n,\alpha}, \Theta_{n,\alpha',\tau}^{\text{slide}})$ for each α . Then we draw the plot of α versus d_α^{hinge} and $d_{\alpha,\tau}^{\text{slide}}$ with $\tau \in \{0.01, 0.1\}$ which is given in the right panel of Figure 2. Note that d_α^{hinge} is large when α is small or large while $d_{\alpha,\tau}^{\text{slide}}$ stays at a lower level regardless of α . That is, the hinge-surrogate fairness constraint does not approximate the original fairness constraint well when α is either small or large and thus the corresponding fair prediction model would be suboptimal. In contrast, the SLIDE-surrogate fairness constraint approximates the original fairness constraint relatively well. This phenomenon is still observed for the two-moon dataset and for DI, whose results are given in Appendix.

4. Theoretical analysis

In this section, we consider the estimated prediction model \hat{f}_n obtained by minimizing the empirical risk $L_n(f)$ on $\mathcal{F}_{n,\alpha+\delta_n,\tau_n}^{\text{slide}} = \{f \in \mathcal{F} : \phi_{n,\tau_n}^{\text{slide}}(f) \leq \alpha + \delta_n\}$ for given τ_n and δ_n converging to 0, and study asymptotic properties of \hat{f}_n . In particular, we derive the upper bound of τ_n such that the fair prediction model with the SLIDE surrogate fairness constraint is asymptotically equivalent to the fair prediction model with the original fairness constraint.

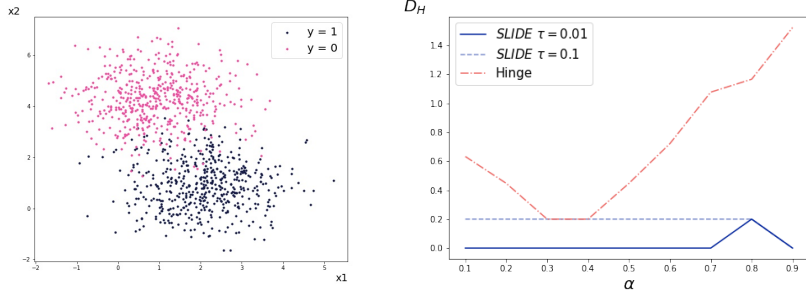


Figure 2: (Left) The scatter plot of the 2-D toy dataset. (Right) Plot of α vs. d_α^{hinge} and $d_{\alpha, \tau}^{\text{slide}}$ for $\tau \in \{0.01, 0.1\}$.

Note that a larger τ_n is better in view of computation since the SLIDE function becomes less non-convex.

For a given estimator \hat{f}_n , we say that the fairness convergence rate of \hat{f}_n is a_n if $\phi(\hat{f}_n) \leq \alpha + a_n$ in probability. Similarly, we say that the l -excess risk convergence rate of \hat{f}_n is b_n if $\mathcal{E}_l(\hat{f}_n, f_\alpha^*) := \mathbf{E}\{l(Y, \hat{f}_n(\mathbf{X}))\} - \mathbf{E}\{l(Y, f_\alpha^*(\mathbf{X}))\} \leq b_n$ in probability, where f_α^* is the true minimizer of $\mathbf{E}\{l(Y, f(\mathbf{X}))\}$ among all measurable functions f with $\phi(f) \leq \alpha$. We derive a_n and b_n in terms of τ_n and δ_n as well as the complexity of \mathcal{F} , that provide a guide to choose τ_n and δ_n . We allow the class of models \mathcal{F} to depend on the sample size, denoted by \mathcal{F}_n , which is popularly used in nonparametric regression contexts to avoid overfitting. For notational simplicity, we drop the subscript n whenever the meaning is clear.

For technical reasons, we derive the fairness and l -excess convergence rates of \hat{f}_n which depend on \hat{f}_n itself. To be more specific, we assume that there exists a constant $M_f > 0$ depending on $f \in \mathcal{F}$ such that

$$|\phi(f) - \phi_{\tau_n}^{\text{slide}}(f)| \leq M_f \tau_n.$$

For example of UIF, we can set $M_f = \sup_{r \in [-\nu, \nu]} g_D(r)$, where g_D is the density of $\sup_{\mathbf{v}: d(\mathbf{X}, \mathbf{v}) \leq \epsilon} D(f(\mathbf{X}), f(\mathbf{v}))$ and ν is a positive constant greater than τ_n . Our convergence rates depend on $M_{\hat{f}_n}$ as well as τ_n .

4.1. Fairness convergence rate

The fairness convergence rate depends on the two quantities: (1) the complexity of \mathcal{F} and (2) the choice of τ_n and δ_n . For the complexity of \mathcal{F} , the empirical Rademacher complexity defined as

$$\widehat{\mathcal{R}}(\mathcal{F}) = \frac{1}{n} \mathbf{E}_{\sigma_i \sim U(\{\pm 1\})^n} \left\{ \sup_{f \in \mathcal{F}} \sum_{i=1}^n \sigma_i f(\mathbf{X}_i) \right\}$$

is a standard measure. The following two theorems show that how the fairness convergence rates depend on τ_n and δ_n as well as the empirical Rademacher complexity.

Theorem 1 (Fairness convergence rate for DI). *When ϕ is DI, the fairness convergence rate of \widehat{f}_n is given by*

$$a_n = \mathcal{O} \left(\delta_n + M_{\widehat{f}_n} \tau_n + \sum_{z \in \{0,1\}} \widehat{\mathcal{R}}_z(\nu_{\tau_n}(\mathcal{F})) + \sqrt{\frac{\log n}{n}} \right),$$

where $\nu_{\tau_n}(\mathcal{F}) := \{\nu_{\tau_n}(f) : f \in \mathcal{F}\}$.

Theorem 2 (Fairness convergence rate for UIF). *When ϕ is UIF with the parameters γ and ϵ , the fairness convergence rate of \widehat{f}_n is given by*

$$a_n = \mathcal{O} \left(\delta_n + M_{\widehat{f}_n} \tau_n + \widehat{\mathcal{R}}(\nu_{\tau_n} \circ \eta(\mathcal{F})) + \sqrt{\frac{\log n}{n}} \right),$$

where $\nu_{\tau_n} \circ \eta(\mathcal{F}) = \{\nu_{\tau_n} \circ \eta_f : f \in \mathcal{F}\}$ and $\eta_f(\mathbf{x}) := D(f(\mathbf{x}), f(\mathbf{x}')) - \gamma$.

Note that the fairness convergence rates in Theorems 1 and 2 cannot be faster by $\sqrt{\log n/n}$. Theorems 1 and 2 imply that the largest τ_n without sacrificing the fairness convergence rate is $\mathcal{O}(\sqrt{\log n/n})$. A situation is similar for δ_n in the sense that $\delta_n = \mathcal{O}(\sqrt{\log n/n})$ makes the fairness constrained space $\mathcal{F}_{n,\alpha+\delta_n,\tau_n}^{\text{slide}}$ be as large as possible without affecting the fairness convergence rate. If the Rademacher complexities are larger than $\mathcal{O}(\sqrt{\log n/n})$, we can let τ_n and δ_n be even larger.

Desirable upper bounds of the Rademacher complexities could not be derived directly from that of \mathcal{F} since the Lipschitz constant of the SLIDE function

ν_{τ_n} diverges as $n \rightarrow \infty$. We calculate the upper bounds of the Rademacher complexities by calculating the metric entropy of $\nu_\tau \circ \eta(\mathcal{F})$ directly. The results for the case of \mathcal{F} being linear model class are provided in Appendix. For deep neural networks, we consider a case where the class \mathcal{F} of prediction models depends on the sample size n and calculate empirical Rademacher complexities to derive (l -excess) risk convergence rates in the following subsection.

4.2. Risk convergence rate

The convergence rate of the (l -excess) risk depends on various choices including the loss function and the model class \mathcal{F} . We use the logistic loss $l(y, f) = \log(1 + \exp(-yf))$. For \mathcal{F} , we consider deep neural networks with the ReLU activation, L_n many layers, N_n many nodes at each layer, S_n many non-zero weights and biases that are bounded by B_n , the final output value being bounded by F_n . To derive the risk convergence rate, we assume that f_α^* belongs to the Hölder space with smoothness ζ (see the definition of Hölder space in Appendix). The next theorem derives the risk convergence rates for DI and UIF as well as the fairness convergence rates.

Theorem 3 (Risk convergence rates for DI and UIF). *Suppose that $n_1/n_0 \rightarrow s \in (0, \infty)$ and that $\phi(f)$ is M -Lipschitz with respect to $\|\cdot\|_\infty$. That is, $|\phi(f_1) - \phi(f_2)| \leq M\|f_1 - f_2\|_\infty$ for some constant $M > 0$. Let $b_n := n^{-\frac{\zeta}{2\zeta+d}}(\log n)^{3/2}$. Moreover, assume that $\delta_n/b_n \rightarrow \infty$ as $n \rightarrow \infty$. Then, for both DI and UIF, there exist positive sequences L_n, N_n, S_n, B_n and F_n such that*

$$\begin{aligned}\mathcal{E}(\hat{f}_n, f_\alpha^*) &\leq \mathcal{O}(b_n + M_{\hat{f}_n} \tau_n) \\ \phi(\hat{f}_n) &\leq \alpha + \mathcal{O}(\delta_n + b_n + M_{\hat{f}_n} \tau_n)\end{aligned}$$

with probability at least $1 - 1/n$.

Assume that $M_{\hat{f}_n}$ is bounded. The largest rate of τ_n that minimizes the risk convergence rate and fairness convergence rate simultaneously is b_n (i.e., $\tau_n = \mathcal{O}(b_n)$), which makes the two convergence rates be almost equal provided δ_n/b_n diverges slowly (e.g., $\log n$ order). This result implies that we can set τ_n

larger when \mathcal{F} is more complex (i.e., ζ is smaller and hence b_n is larger) and vice versa.

For standard classification problems, the risk convergence rate could be faster than $1/\sqrt{n}$ and hence the risk convergence rate in Theorem 3 looks sub-optimal. However, this slower convergence rate is unavoidable since f_α^* is not the global minimizer of the population risk $\mathbf{E}\{l(Y, f(\mathbf{X}))\}$ among all measurable functions. We believe that the risk convergence rate in Theorem 3 would be optimal.

4.3. Remarks on $M_{\hat{f}_n}$

The convergence rates in Theorems 1, 2 and 3 would be meaningful only if $M_{\hat{f}_n}$ is not too large (i.e. bounded). Let $\tau_n = \mathcal{O}(b_n)$, which is the largest τ_n that does not change the convergence rates. In Proposition 1 of Appendix, we prove that $M_{\hat{f}_n} \leq M_{n, \hat{f}_n} + \mathcal{O}(1)$, where

$$M_{n,f} = |\phi_{n,-\tau_n}^{\text{slide}}(f; \gamma, \epsilon) - \phi_{n,\tau_n}^{\text{slide}}(f; \gamma, \epsilon)|/\tau_n$$

for UIF, where $\phi_{n,-\tau_n}^{\text{slide}}$ is the opposite SLIDE-surrogate fairness constraint (i.e., ν_τ in $\phi_{n,\tau_n}^{\text{slide}}$ is replaced by $\nu_{-\tau} = \frac{z}{\tau} \mathbb{I}(-\tau < z \leq 0) + \mathbb{I}(z > 0)$). The population version of $\phi_{-\tau_n}^{\text{slide}}$ can be defined similarly. A formula of $M_{n,f}$ for DI is provided in Proposition 2 of Appendix. Thus, when M_{n, \hat{f}_n} is not large, we expect that $M_{\hat{f}_n}$ is also small.

The above result provides a way of using the SLIDE-surrogate fairness constraint in practice. First, we learn f by \hat{f}_n with the SLIDE-surrogate fairness constraint. Then, if M_{n, \hat{f}_n} is not too large, we keep using \hat{f}_n for prediction. Otherwise, we abort \hat{f}_n and resort to other fairness AI algorithms. For the datasets analyzed in our numerical experiments, M_{n, \hat{f}_n} is not larger than 0.5 so that we decide to keep using the SLIDE-surrogate fairness constraints in our experiments.

5. Experiments

We compare the SLIDE-surrogate fairness constraints with the hinge-surrogate fairness constraints by analyzing three benchmark datasets. For the class of models, we use one hidden layer deep neural networks. We utilize the Pytorch framework with NVIDIA TITAN RTX GPUs. Details about learning algorithms are described in Appendix.

Datasets. We analyze three public datasets popularly used in fairness AI: (1) *Adult* dataset [47], (2) *Bank* dataset from UCI [48], and (3) *Law* dataset¹. They have gender, age and race as the sensitive variable, respectively. For each dataset, we split the whole dataset into training, validation and test datasets with ratio 60% : 20% : 20% randomly and repeat this random splitting three times. We choose the regularization parameters on validation data and assess the performances (accuracy and level of fairness) on test data.

Performance measures. For prediction accuracy, we use two measures: accuracy (Acc) and balanced accuracy (BA). The balanced accuracy, which is considered by [49, 44], is an average of the accuracies in each class of label $y = -1$ and $y = 1$. For assessing fairness, we calculate DI on test data for group fairness. For individual fairness, we use the consistency (Con.) of prediction considered by [49, 44]. ‘Con.’ measures how frequently the predictive class labels of two inputs that are the same except the sensitive variable coincide. Note that a larger value of ‘Con.’ means that the prediction model is more individually fair.

Optimization algorithms. To learn a fair prediction model, we minimize $L_n(f) + \lambda\phi_n(f)$ on $f \in \mathcal{F}$ for a given surrogate fairness constraint ϕ_n , where λ is the Lagrangian multiplier. For λ , we fix the accuracy at a certain level and choose λ such that the accuracy of $\hat{f}_{n,\lambda}$, a (local) minimizer of $L_n(f) + \lambda\phi_n(f)$, on the validation data is closest to the fixed accuracy. Then, we compare the

¹<http://www.seaphe.org/databases.php>

level of fairness. Since deep neural networks and the SLIDE function are highly non-linear, we train multiple models with multiple random initial parameters and then select the most fair model. We use the Adam algorithm [50] for the optimization.

For the SLIDE-surrogate, we try another optimization algorithm where the solutions obtained with the hinge-surrogate fairness constraint are used as initial solutions, which we call the hybrid SLIDE (HySLIDE) algorithm. By comparing the SLIDE (a gradient descent algorithm with random initials) and HySLIDE, we can investigate how sensitive the SLIDE-surrogate fairness constraint is to the choice of initials. In addition, we apply the CCCP to the SLIDE-surrogate UIF, whose details and results are provided in Appendix.

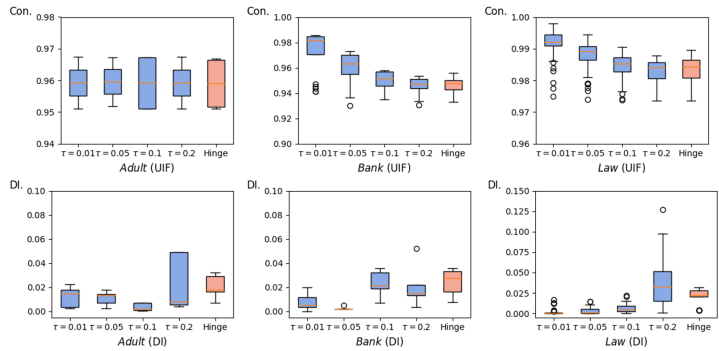


Figure 3: Box plots of levels of fairness (Con. and DI.) of fair prediction models learned by the SLIDE with $\tau \in \{0.01, 0.05, 0.1, 0.2\}$ and the hinge for the three datasets.

Figure 3 draws the box plots of the levels of fairness of the fair prediction models learned with the SLIDE- and hinge- surrogate fairness constraints. The implication of Figure 3 is that performance of the SLIDE does not strongly depend on the value of τ as long as τ lies in a reasonable range (i.e., $(0.01, 0.2)$). The SLIDE-surrogate fairness constraint has one more regularization parameter τ compared to the hinge-surrogate fairness constraint. To make the comparison fair, we select τ randomly from $(0.01, 0.2)$ along with a random initial solution. For the hinge-surrogate fairness constraint, we learn multiple prediction models corresponding to multiple random initial parameters and choose

the most fair model among those whose accuracies on the validation dataset are similar to a priori given accuracy. Similarly, for the SLIDE-surrogate fairness constraint, we learn multiple prediction models corresponding to multiple pairs of randomly selected τ and randomly selected initial parameters and choose the most fair model.

5.1. Group fairness

We compare the SLIDE-surrogate and hinge-surrogate fairness constraints for DI. Table 1 summarizes the results, which indicate that the SLIDE-surrogate fairness constraint performs better than the hinge-surrogate fairness constraint for DI.

Dataset	Method	Acc	BA	DI
<i>Adult</i>	DI + Hinge	82.80	72.34	.013 (.001)
	DI + SLIDE	82.19	72.14	.007 (.003)
	DI + HySLIDE	82.24	72.33	.010 (.002)
<i>Bank</i>	DI + Hinge	90.07	73.33	.015 (.002)
	DI + SLIDE	90.24	73.22	.013 (.002)
	DI + HySLIDE	90.01	73.42	.016 (.003)
<i>Law</i>	DI + Hinge	82.51	59.24	.013 (.004)
	DI + SLIDE	82.49	58.99	.008 (.003)
	DI + HySLIDE	82.41	59.54	.014 (.003)

Table 1: The performances (Acc(%), BA(%), DI) of group-fair prediction models on *Adult*, *Bank* and *Law* test datasets.

Furthermore, we compare the SLIDE-surrogate fairness constraint with other state-of-the-art methods, [20] and [40] in Table 2. The SLIDE-surrogate fairness constraint outperforms the other competitors.

5.2. Individual fairness

Table 3 compares the SLIDE-surrogate and the hinge-surrogate fairness constraints, which also confirms that the SLIDE is superior to the hinge. Figure 4

Dataset	Method	Acc	BA	DI
<i>Adult</i>	[20]	82.11	72.50	.018 (.003)
	[40]	82.09	72.05	.016 (.003)
	DI + SLIDE	82.19	72.14	.007 (.003)
<i>Bank</i>	[20]	90.04	73.41	.029 (.004)
	[40]	89.35	73.35	.016 (.002)
	DI + SLIDE	90.24	73.22	.013 (.002)
<i>Law</i>	[20]	82.50	58.95	.020 (.003)
	[40]	82.40	58.83	.014 (.001)
	DI + SLIDE	82.49	58.99	.008 (.003)

Table 2: Group fairness (DI) fairness performances (Acc(%), BA(%), DI) with state-of-the-art baseline methods [20] and [40] on the *Adult*, *Bank* and *Law* test datasets.

draws the Pareto front plots of the accuracy and the balanced accuracy versus a level of fairness (Con.) for the *Adult* dataset, which clearly shows that the SLIDE-surrogate fairness constraint uniformly dominates the hinge-surrogate fairness constraint.

Table 4 compares two other individual fairness learning algorithms - SenSR [49] and SenSeI [44] with the surrogate UIF constraints. Here, we follow the data pre-processing and regularization parameter selection technique used in [49] and [44]. In Table 4, ‘S-Con.’ is the consistency value when the variable “spouse” is changed and ‘GR-con.’ is the consistency value when the variables “gender” and “race” are changed [49, 44]. For these two fairness measures, the SLIDE-surrogate fairness constraint performs better than SenSR and SenSeI as well as the hinge-surrogate fairness constraint.

6. Conclusion and discussion

The main message of this paper is to show that using the hinge function as a surrogate function of the indicator function in the fairness constraint does not work. Thus, we need to be careful to choose a surrogate function of the indica-

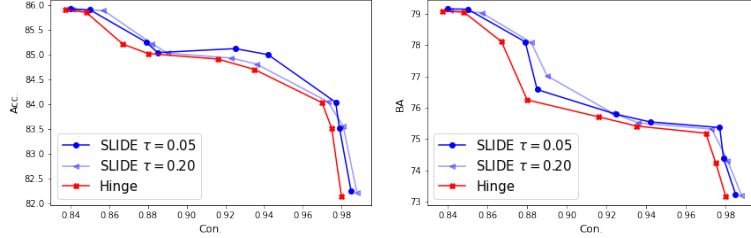


Figure 4: Fairness vs. Accuracy on *Adult* dataset. (Left): Pareto front plot of (Con., Acc.). (Right): Pareto front plot of (Con., BA.). Blue lines are those for the SLIDE-surrogate with different $\tau = 0.05, 0.20$, and the orange line is for the hinge-surrogate.

Dataset	Method	Acc	BA	Con.
<i>Adult</i>	UIF + Hinge	84.60	75.75	.916 (.003)
	UIF + SLIDE	84.36	75.73	.920 (.005)
	UIF + HySLIDE	84.51	75.69	.922 (.003)
<i>Bank</i>	UIF + Hinge	90.29	63.82	.985 (.006)
	UIF + SLIDE	90.14	63.43	.990 (.005)
	UIF + HySLIDE	90.15	63.03	.984 (.004)
<i>Law</i>	UIF + Hinge	83.75	62.67	.985 (.006)
	UIF + SLIDE	83.99	62.71	.986 (.004)
	UIF + HySLIDE	84.02	62.79	.987 (.003)

Table 3: Performances (Acc(%), BA(%), Con.) of individually fair prediction models on *Adult*, *Bank* and *Law* test datasets.

tor function and the choice should depend on the context of a given problem.

By closely investigating the gradient of the SLIDE-surrogate fairness constraint, we find an interesting new group fairness constraint so called the *DI-boundary* defined as $\phi^{\text{DI-bound}}(f) = |\mathbf{P}\{0 \leq f(\mathbf{X}) \leq \tau | Z = 0\} - \mathbf{P}\{0 \leq f(\mathbf{X}) \leq \tau | Z = 1\}|$. The DI-boundary requires fairness only for individuals whose scores are around the decision boundary. That is, when the fairness of f is assessed, individuals who have very large scores (i.e., super-performers if a larger value of f means a higher ability) are excluded from the analysis. If we replace the indicator function in $\phi^{\text{DI-bound}}(f)$ by the hinge function, the gradient of the hinge-

<i>Adult</i>	Acc	BA	S-Con.	GR-Con.
UIF + Hinge	85.3	76.8	.936	.967
UIF + SLIDE	85.1	76.6	.970	.985
UIF + HySLIDE	85.2	76.6	.976	.981
SenSeI	-	76.8	.945	.963
SenSR	78.7	78.9	.934	.984

Table 4: Performances (Acc(%), BA(%), S-Con., and GR-Con.) of individually fair prediction models on *Adult* test dataset. For SenSeI [44] and SenSR [49], we copied the results from [44].

surrogate DI-boundary is equal proportional to the gradient of the SLIDE-surrogate DI provided that $0 \leq f(\mathbf{X}) \leq \tau$ is replaced by $0 \leq f^{\text{curr}}(\mathbf{X}) \leq \tau$, where f^{curr} is the current solution. Most existing fairness constraints require a prediction model fair for all individuals. It would be useful to think about the concept of partial fairness where f is fair only for a specific subset of the population.

Acknowledgements

This work was supported by Institute for Information & communications Technology Planning & Evaluation(IITP) grant funded by the Korea government(MSIT) (No. 2019-0-01396, Development of framework for analyzing, detecting, mitigating of bias in AI model and training data).

Supplementary materials of SLIDE: A surrogate fairness constraint to ensure fairness-consistency

In this supplement, we present (i) the proofs of Theorems 1, 2 and 3 in Sections A, B and C, (ii) details of experiments in Section D and (iii) results of additional experiments in Section E.

Appendix

A. Notations and definitions

Denote the compact domain of inputs as $\mathcal{X} \subset \mathbb{R}^d$. For a given function f , we let $\|\cdot\|_p$ be the l_p norm defined as $\|f\|_p := \left(\int_{\mathcal{X}} |f(\mathbf{x})|^p d\mu(\mathbf{x})\right)^{1/p}$ where μ is the Lebesgue measure on \mathbb{R}^d . In addition, we let $\|f\|_{\infty} := \sup_{\mathbf{x} \in \mathcal{X}} |f(\mathbf{x})|$.

For a given $\alpha > 0$, $[\alpha]$ is the largest integer less than or equal to α and $\lceil \alpha \rceil$ is the smallest integer greater or equal to α . For given $\mathbf{s} = [s_1, \dots, s_d]^{\top} \in \mathbb{N}_0^d$, where \mathbb{N}_0 is the set of nonnegative integers, we define the derivative of f of order \mathbf{s} as

$$\partial^{\mathbf{s}} f = \frac{\partial^{|\mathbf{s}|} f}{\partial x_1^{s_1} \cdots \partial x_d^{s_d}},$$

where $|\mathbf{s}| = s_1 + \cdots + s_d$. Further, we let

$$[f]_{r, \mathcal{X}} = \sup_{\mathbf{x}, \mathbf{x}' \in \mathcal{X}, \mathbf{x} \neq \mathbf{x}'} \frac{|f(\mathbf{x}) - f(\mathbf{x}')|}{|\mathbf{x} - \mathbf{x}'|^r}$$

for $r \in (0, 1]$.

Definition 1 (Smooth functions). *For $m \in \mathbb{N}$, we denote $C^m(\mathcal{X})$ as the space of m -times differentiable functions on \mathcal{X} as whose partial derivatives of order \mathbf{s} with $|\mathbf{s}| \leq m$ are continuous. That is,*

$$C^m(\mathcal{X}) = \{f : \mathcal{X} \rightarrow \mathbb{R}, \partial^{\mathbf{s}} f \text{ are continuous for } \forall \mathbf{s} \text{ such that } |\mathbf{s}| \leq m\}.$$

Definition 2 (Hölder space). *Hölder space with smoothness $\zeta > 0$ is a function space defined as*

$$\mathcal{H}^{\zeta}(\mathcal{X}) := \{f \in C^{[\zeta]}(\mathcal{X}) : \|f\|_{\mathcal{H}^{\zeta}(\mathcal{X})} < \infty\}$$

where $\|f\|_{\mathcal{H}^\zeta(\mathcal{X})} = \max_{|\mathbf{m}| \leq [\zeta]} \|\partial^{\mathbf{m}} f\|_{\infty, \mathcal{X}} + \max_{|\mathbf{m}| = [\zeta]} [\partial^{\mathbf{m}} f]_{\zeta_0, \mathcal{X}}$.

Definition 3 (The ϵ -covering number). *The ϵ -covering number of a given class of functions \mathcal{F} is the cardinality of the minimal ϵ -covering set of \mathcal{F} with respect to the L_p norm, which is defined as:*

$$N(\epsilon, \mathcal{F}, \|\cdot\|_p) := \inf\{n \in \mathbb{N} : \exists f_1, \dots, f_n \text{ s.t. } \mathcal{F} \subset \bigcup_{i=1}^n B_p(f_i, \epsilon)\},$$

where $B_p(f_i, \epsilon) := \{f \in \mathcal{F} : \|f - f_i\|_p \leq \epsilon\}$.

Definition 4 (Metric entropy). *The (ϵ -) metric entropy of \mathcal{F} (w.r.t. L_p norm) is a logarithm of the ϵ -covering number of \mathcal{F} (w.r.t. L_p norm), i.e.,*

$$H(\epsilon, \mathcal{F}, \|\cdot\|_p) := \log(N(\epsilon, \mathcal{F}, \|\cdot\|_p)).$$

Definition 5 (Rademacher complexity). *Let σ be a random variable having -1 or 1 with probability 1/2 each. For independent realizations $\sigma_1, \dots, \sigma_n$ of σ , we define the empirical Rademacher complexity of a function class \mathcal{F} as*

$$\widehat{\mathcal{R}}(\mathcal{F}) := \frac{1}{n} \mathbf{E}_\sigma \left\{ \sup_{f \in \mathcal{F}} \sum_{i=1}^n \sigma_i f(\mathbf{X}_i) \right\}.$$

The Rademacher complexity is the expectation of the empirical one with respect to \mathbf{X} .

That is, the (population) Rademacher complexity of \mathcal{F} is

$$\mathcal{R}(\mathcal{F}) := \mathbf{E}_{\mathbf{X}} \{ \widehat{\mathcal{R}}(\mathcal{F}) \}.$$

B. Technical lemmas

This section introduces technical lemmas used to prove the Theorems 1, 2 and 3. Particularly, Lemma 5 provides a tight upper bound of $\widehat{\mathcal{R}}(\nu_\tau(\mathcal{F}))$ when \mathcal{F} is class of deep neural networks, which plays a key role in deriving the convergence rates. In addition, even though we do not derive the convergence rates, we demonstrate how to obtain a tight upper bound of $\widehat{\mathcal{R}}(\nu_\tau(\mathcal{F}))$ when \mathcal{F} is a class of linear functions in Example 1. For technical simplicity, we assume that the distribution of \mathbf{X} has a density $p(\mathbf{x})$ such that $0 < \inf_{\mathbf{x} \in \mathcal{X}} p(\mathbf{x}) \leq \sup_{\mathbf{x} \in \mathcal{X}} p(\mathbf{x}) < \infty$.

Lemma 1. Let $\eta_f(\mathbf{x}) := D(f(\mathbf{x}), f(\mathbf{x}')) - \gamma$ with a Lipschitz (on bounded domain) metric $D(\cdot, \cdot)$ for a given $\gamma > 0$. Then, there exists $c > 0$ such that

$$\|\eta_{f_1} - \eta_{f_2}\|_\infty \leq c\|f_1 - f_2\|_\infty$$

for any two functions f_1 and f_2 .

Lemma 2 (Theorem 26.5 of [51]). Let \mathcal{H} be a set of real-valued functions such that $\|l \circ h\|_\infty \leq H$ for any $h \in \mathcal{H}$ for some $H > 0$. Then,

$$L_P(h) \leq L_n(h) + 2\widehat{\mathcal{R}}_n(l \circ \mathcal{H}) + 4H\sqrt{\frac{2\log(4/\delta)}{n}}$$

for any $h \in \mathcal{H}$, with probability at least $1 - \delta > 0$.

Lemma 3 (Dudley's Theorem (Theorem 1.19 of [52])). Let \mathcal{H} be a set of real-valued functions such that $\|h\|_\infty \leq H$ for any $h \in \mathcal{H}$ for some $H > 0$. Then,

$$\widehat{\mathcal{R}}(\mathcal{H}) \leq \inf_{\alpha \in [0, H/2)} \left(4\alpha + \frac{12}{\sqrt{n}} \int_\alpha^H \sqrt{\log \mathcal{N}(\epsilon, \mathcal{H}, \|\cdot\|_{n,2})} d\epsilon \right) \quad (6)$$

where $\|\cdot\|_{n,2}$ denotes the empirical L_2 norm defined by $\|h\|_{n,2} := \sqrt{n^{-1} \sum_{i=1}^n h(\mathbf{X}_i)^2}$ for $h \in \mathcal{H}$.

Lemma 4 (Lemma 3 of [53]). Let \mathcal{F} be a set of deep neural networks with the ReLU activation function, L many layers, N many nodes at each layer, S many nonzero weights and biases that are bounded by B . Then for any $\epsilon > 0$,

$$\log \mathcal{N}(\epsilon, \mathcal{F}, \|\cdot\|_\infty) \leq 2S(L+1) \log \left(\frac{(L+1)(N+1)B}{\epsilon} \right). \quad (7)$$

Lemma 5. Let $g : \mathbb{R} \rightarrow \mathbb{R}$ be a Lipschitz function in a sense that $|g(z_1) - g(z_2)| \leq C'|z_1 - z_2|$ for any $z_1, z_2 \in \mathbb{R}$ for some constant $C' > 0$. Let \mathcal{F} be a set of deep neural networks with the ReLU activation function, L many layers, N many nodes at each layer, S many nonzero weights and biases that are bounded by B . Let $g(\mathcal{F}) := \{g(f) : f \in \mathcal{F}\}$ and $F' = \sup_{f \in \mathcal{F}} \|g(f)\|_\infty$. Then

$$\widehat{\mathcal{R}}(g(\mathcal{F})) \leq \frac{4}{n} + \frac{12F'}{\sqrt{n}} \sqrt{S(L+1) \log(C'n(L+1)(N+1)B)}.$$

The next two propositions compute $M_{n,f}$ for UIF and DI.

Proposition 1 (Upper bound of M_f for UIF). *Let \mathcal{F} be the class of DNN models considered in Theorem 3. Suppose $\tau_n = \mathcal{O}(b_n)$, where b_n is the sequence defined in Theorem 3. Then we have*

$$M_f \leq \frac{1}{\tau_n} |\phi_{n,-\tau_n}^{\text{slide}}(f; \gamma, \epsilon) - \phi_{n,\tau_n}^{\text{slide}}(f; \gamma, \epsilon)| + \mathcal{O}(1)$$

for all $f \in \mathcal{F}$.

Proposition 2 (Upper bound of M_f for DI). *Let \mathcal{F} be the class of DNN models considered in Theorem 3. Suppose $\tau_n = \mathcal{O}(b_n)$, where b_n is the sequence defined in Theorem 3. Then we have*

$$M_f \leq \frac{1}{\tau_n} \left(\sum_{z=0,1} \left| \frac{1}{n_z} \sum_{z_i=z} \left(\nu_{-\tau_n}(f(\mathbf{x}_i)) - \nu_{\tau_n}^{\text{slide}}(f(\mathbf{x}_i)) \right) \right| + |\phi_{n,\tau_n}^{\text{slide}}(f) - \phi_n(f)| \right) + \mathcal{O}(1)$$

for all $f \in \mathcal{F}$.

Obtaining a tight upper bound of the Rademacher complexity plays a key role to derive a fast convergence rate. We need an upper bound of $\widehat{\mathcal{R}}(\nu_\tau(\mathcal{F}))$ while that of $\widehat{\mathcal{R}}(\mathcal{F})$ is well known for many classes of \mathcal{F} . Since ν_τ is $1/\tau$ -Lipschitz, we may use the inequality $\widehat{\mathcal{R}}(\nu_\tau(\mathcal{F})) \leq \widehat{\mathcal{R}}(\mathcal{F})/\tau$ to derive an upper bound. However, such a naive approach would not yield a good upper bound in particular when τ converges to 0 as n increases. For deep neural networks, we derive an upper bound in Lemma 5 by directly calculating the corresponding metric entropy. In the following example, we illustrate how to derive a good upper bound of the Rademacher complexity when \mathcal{F} is a class of linear functions. In particular, we derive an upper bound of the L_2 -metric entropy of $\nu_\tau(\mathcal{F})$, with which we could obtain an upper bound of the Rademacher complexity by use of Lemma 3.

Example 1 (Linear model $\mathcal{F}^{\text{linear}}$). *Let $\mathcal{F}^{\text{linear}} = \{\langle \mathbf{w}, \cdot \rangle : \mathbf{w} \in \mathbb{R}^d, \|\mathbf{w}\|_2 \leq B\}$. Since ν_τ is $1/\tau$ -Lipschitz, we have $\mathcal{N}(\epsilon, \nu_\tau(\mathcal{F}^{\text{linear}}), \|\cdot\|_2) \leq \mathcal{N}(\epsilon\tau, \mathcal{F}^{\text{linear}}, \|\cdot\|_\infty)$. Finally, we can obtain the bound of the entropy as $\log \mathcal{N}(\epsilon\tau_n, \mathcal{F}^{\text{linear}}, \|\cdot\|_\infty) \leq d \log \left(\frac{C}{\epsilon\tau_n} \right)$ for some $C > 0$ and $\tau = \tau_n$ by Lemma 2.5 of [54]. Hence, the Rademacher complexity of $\nu_{\tau_n}(\mathcal{F}^{\text{linear}})$ is bounded by (asymptotically) $\log(1/\tau_n)$ but not $1/\tau_n$.*

C. Proofs

This section presents the proofs of Lemmas 1 and 5, Theorems 1, 2 and 3, and Propositions 1 and 2.

Proof of Lemma 1.

Proof. By the Lipschitz property of D , there exists a constant $C > 0$ such that $D(z, z') \leq C|z - z'|$ for all $z, z' \in \{x \in \mathbb{R} : |x| \leq K\}$, which is a bounded domain, for a given $K > 0$.

Denote

$$\mathbf{x}'_{f_1} := \arg \max_{\mathbf{x}' : d(\mathbf{x}, \mathbf{x}') \leq \epsilon} D(f_1(\mathbf{x}), f_1(\mathbf{x}'))$$

and

$$\mathbf{x}'_{f_2} := \arg \max_{\mathbf{x}' : d(\mathbf{x}, \mathbf{x}') \leq \epsilon} D(f_2(\mathbf{x}), f_2(\mathbf{x}')).$$

Then, we consider any metric as the similarity measure $D(\cdot, \cdot)$ between prediction values, we can write $|\eta_{f_1}(\mathbf{x}) - \eta_{f_2}(\mathbf{x})| = |D(f_1(\mathbf{x}), f_1(\mathbf{x}'_{f_1})) - D(f_2(\mathbf{x}), f_2(\mathbf{x}'_{f_2}))|$.

(Case 1) $D(f_1(\mathbf{x}), f_1(\mathbf{x}'_{f_1})) \geq D(f_2(\mathbf{x}), f_2(\mathbf{x}'_{f_2}))$: Then,

$$\begin{aligned} |\eta_{f_1}(\mathbf{x}) - \eta_{f_2}(\mathbf{x})| &= |D(f_1(\mathbf{x}), f_1(\mathbf{x}'_{f_1})) - D(f_2(\mathbf{x}), f_2(\mathbf{x}'_{f_2}))| \\ &\leq |D(f_1(\mathbf{x}), f_1(\mathbf{x}'_{f_1})) - D(f_2(\mathbf{x}), f_2(\mathbf{x}'_{f_1}))| \\ &\leq |D(f_1(\mathbf{x}), f_1(\mathbf{x}'_{f_1})) - D(f_2(\mathbf{x}), f_2(\mathbf{x}'_{f_1}))| \\ &\leq |D(f_1(\mathbf{x}), f_2(\mathbf{x})) + D(f_1(\mathbf{x}'_{f_1}), f_2(\mathbf{x}'_{f_1}))|. \end{aligned}$$

The first inequality holds since $D(f_2(\mathbf{x}), f_2(\mathbf{x}'_{f_2})) \geq D(f_2(\mathbf{x}), f_2(\mathbf{x}'))$ for all \mathbf{x}' .

(Case 2) $D(f_1(\mathbf{x}), f_1(\mathbf{x}'_{f_1})) \leq D(f_2(\mathbf{x}), f_2(\mathbf{x}'_{f_2}))$: We can derive $|\eta_{f_1}(\mathbf{x}) - \eta_{f_2}(\mathbf{x})| \leq |D(f_1(\mathbf{x}), f_2(\mathbf{x})) + D(f_1(\mathbf{x}'_{f_2}), f_2(\mathbf{x}'_{f_2}))|$ similarly. Since the two inequalities hold for any \mathbf{x} and D is Lipschitz, we can take supremum for each hand-side to obtain the desired result as

$$\|\eta_{f_1} - \eta_{f_2}\|_\infty \leq c \cdot \|f_1 - f_2\|_\infty$$

for $c > 0$ that depends on the Lipschitz constant C .

□

Proof of Lemma 5.

Proof. By the Lipschitz property of g , we have $\|g(f_1) - g(f_2)\|_{n,2}^2 = \frac{1}{n} \sum_{i=1}^n |g(f_1(\mathbf{x}_i)) - g(f_2(\mathbf{x}_i))|^2 \leq (C')^2 \|f_1 - f_2\|_\infty^2$ and thus $\mathcal{N}(\epsilon, g(\mathcal{F}), \|\cdot\|_{n,2}) \leq \mathcal{N}(\epsilon/C', \mathcal{F}, \|\cdot\|_\infty)$.

Then by Lemma 4, the integral term in Lemma 3 is bounded as

$$\begin{aligned} \int_\alpha^{F'} \sqrt{\log \mathcal{N}(u/C', \mathcal{F}, \|\cdot\|_\infty)} d\epsilon &\leq F' \sqrt{\log \mathcal{N}(\alpha/C', \mathcal{F}, \|\cdot\|_\infty)} \\ &\leq F' \sqrt{2S(L+1) \log \left(\frac{C'(L+1)(N+1)B}{\alpha} \right)}. \end{aligned}$$

Taking $\alpha = 1/n$ completes the proof. \square

Proof of Theorem 1.

Proof. Let

$$\phi_{\tau_n}^{\text{slide}}(f) = |\mathbf{E}\{\nu_{\tau_n}(f(\mathbf{X}))|Z=0\} - \mathbf{E}\{\nu_{\tau_n}(f(\mathbf{X}))|Z=1\}|.$$

Then using the inequality $|a| - |b| \leq |a - b|$, we have

$$\begin{aligned} &|\phi_{n,\tau_n}^{\text{slide}}(\hat{f}_n) - \phi(\hat{f}_n)| \\ &\leq \sum_{z \in \{0,1\}} \left| \frac{1}{n_z} \sum_{i:z_i=z} \nu_{\tau_n}(\hat{f}_n(\mathbf{x}_i)) - \mathbf{E}\{\nu_{\tau_n}(\hat{f}_n(\mathbf{X}))|Z=z\} \right| + |\phi_{\tau_n}^{\text{slide}}(\hat{f}_n) - \phi(\hat{f}_n)|. \end{aligned}$$

Since the SLIDE function ν_{τ_n} is bounded in $[0, 1]$, by Lemma 2 the first term of the right-hand side of the preceding display is bounded by

$$\sum_{z \in \{0,1\}} \left(\widehat{\mathcal{R}}_z(\nu_{\tau_n}(\mathcal{F})) + 4\sqrt{\frac{2 \log(8n)}{n_z}} \right)$$

with probability at least $1 - 1/n$. On the other hand, the second term of the right-hand side is bounded by $M_{\hat{f}_n} \tau_n$ by the definition of M_f . By the assumptions $n_1/n_0 \rightarrow s \in (0, \infty)$, we have

$$\begin{aligned} \phi(\hat{f}_n) &\leq \phi_{n,\tau_n}^{\text{slide}}(\hat{f}_n) + |\phi_{n,\tau_n}^{\text{slide}}(\hat{f}_n) - \phi(\hat{f}_n)| \\ &\leq \alpha + \delta_n + C \left(\sum_{z \in \{0,1\}} \widehat{\mathcal{R}}_z(\nu_{\tau_n}(\mathcal{F})) + \sqrt{\frac{\log n}{n}} \right) + M_{\hat{f}_n} \tau_n \end{aligned}$$

for some constant $C > 0$ with probability at least $1 - 1/n$, which completes the proof. \square

Proof of Theorem 2.

Proof. Let $\phi_{\tau_n}^{\text{slide}}(f; \gamma, \epsilon) = \mathbb{E}\{\nu_{\tau_n} \circ \eta_f\}$. Since the SLIDE function ν_{τ_n} is bounded in $[0, 1]$, Lemma 2 implies that

$$\begin{aligned} & \left| \phi_{n, \tau_n}^{\text{slide}}(\hat{f}_n; \gamma, \epsilon) - \phi(\hat{f}_n; \gamma, \epsilon) \right| \\ & \leq \left| \phi_{n, \tau_n}^{\text{slide}}(\hat{f}_n; \gamma, \epsilon) - \phi_{\tau_n}^{\text{slide}}(\hat{f}_n; \gamma, \epsilon) \right| + \left| \phi_{\tau_n}^{\text{slide}}(\hat{f}_n; \gamma, \epsilon) - \phi(\hat{f}_n; \gamma, \epsilon) \right| \\ & \leq 2\hat{\mathcal{R}}(\nu_{\tau_n} \circ \eta(\mathcal{F})) + 4\sqrt{\frac{2\log(4n)}{n}} + M_{\hat{f}_n} \tau_n \end{aligned}$$

with probability at least $1 - 1/n$, which completes the proof. \square

Proof of Theorem 3.

Proof. We prove Theorem 3 for DI and UIF separately.

Case 1: DI

Since f_α^* is a Hölder smooth function with smoothness $\zeta > 0$, by Theorem 5 of [55], for any sufficiently large n , there is a neural network $f_n^* \in \mathcal{F}$ such that

$$\|f_n^* - f_\alpha^*\|_\infty \leq C'_1 n^{-\frac{\zeta}{2\zeta+d}} =: b'_n$$

for some absolute constant $C'_1 > 0$, provided that $L_n = L_0 \log n$, $N_n = N_0 n^{\frac{d}{2\zeta+d}}$, $S_n = S_0 n^{\frac{d}{2\zeta+d}} \log n$, $B_n = 1$ and $F_n = F_0 \geq \|f_\alpha^*\|_\infty$, where L_0 , N_0 , S_0 and F_0 are constants depending only on d and ζ . From now on, we assume that the set \mathcal{F} include all deep neural networks of the architectures satisfying the above conditions. By the Lipschitz property of ϕ , we have

$$\phi(f_n^*) \leq \phi(f_\alpha^*) + L\|f_n^* - f_\alpha^*\|_\infty \leq \alpha + Mb'_n$$

i.e., $f_n^* \in \mathcal{F}_{\alpha+Mb'_n}$. Define the event

$$\mathcal{E}_n(\xi) := \left\{ \{(Y_i, \mathbf{X}_i)\}_{i=1}^n : \sup_{f \in \mathcal{F}} \left| \phi_{n, \tau_n}^{\text{slide}}(f) - \phi(f) \right| \leq \xi \right\}$$

for $\xi > 0$. Let

$$\phi_{\tau_n}^{\text{slide}}(f) = |\mathbf{E}(\nu_{\tau_n}(f(\mathbf{X}))|Z=0) - \mathbf{E}(\nu_{\tau_n}(f(\mathbf{X}))|Z=1)|.$$

Then using the inequality $|a| - |b| \leq |a - b|$, we get

$$\begin{aligned} & \left| \phi_{n, \tau_n}^{\text{slide}}(\hat{f}_n) - \phi(\hat{f}_n) \right| \\ & \leq \sum_{z \in \{0,1\}} \left| \frac{1}{n_z} \sum_{i:z_i=z} \nu_{\tau_n}(\hat{f}_n(\mathbf{x}_i)) - \mathbf{E}(\nu_{\tau_n}(\hat{f}_n(\mathbf{X}))) | Z = z \right| + |\phi_{\tau_n}^{\text{slide}}(\hat{f}_n) - \phi(\hat{f}_n)|. \end{aligned}$$

Since the SLIDE function ν_{τ_n} is $1/\tau_n$ -Lipschitz and bounded in $[0, 1]$, by Lemmas 2 and 5, the first term of the right-hand side of the preceding display is bounded as

$$\begin{aligned} & \sum_{z \in \{0,1\}} \left(\frac{8}{n_z} + \frac{24}{\sqrt{n_z}} \sqrt{S_n(L_n + 1) \log(n(L_n + 1)(N_n + 1)B_n)/\tau_n} + 4\sqrt{\frac{2 \log(4/\delta)}{n_z}} \right) \\ & \leq C'_2 \sum_{z \in \{0,1\}} \left(\frac{1}{n_z} + \frac{1}{\sqrt{n_z}} \sqrt{n^{\frac{p}{2\zeta+p}} (\log n)^3} + \sqrt{\frac{\log(1/\delta)}{n_z}} \right) \end{aligned}$$

for some constant $C'_2 > 0$ with probability at least $1 - 2\delta$. On the other hand, the second term of the right-hand side is bounded by $M_{\hat{f}_n} \tau_n$ by the definition of M_f . Hence, by the assumptions $n_1/n_0 \rightarrow s \in (0, \infty)$, we have by taking $\delta = 1/(8n)$,

$$\left| \phi_{n, \tau_n}^{\text{slide}}(\hat{f}_n) - \phi(\hat{f}_n) \right| \leq C'_3 \left(n^{-\frac{\zeta}{2\zeta+p}} (\log n)^{3/2} \right) = C'_3 b_n + M_{\hat{f}_n} \tau_n$$

for some constant $C'_3 > 0$ with probability at least $1 - 1/(4n)$. That is, $\mathbf{P}\{\mathcal{E}_n(C'_3 b_n + M_{\hat{f}_n} \tau_n)^c\} \leq 1/(4n)$.

Now we show that the convergence rate of $\mathcal{E}(\hat{f}_n, f_n^*)$ on $\mathcal{E}_n(C'_3 b_n + M_{\hat{f}_n} \tau_n)$. Firstly we note that $f_n^* \in \mathcal{F}_{n, \alpha+Mb'_n+C'_3 b_n+M_{\hat{f}_n} \tau_n, \tau_n}^{\text{slide}}$ on $\mathcal{E}(C'_3 b_n + M_{\hat{f}_n} \tau_n)$.

Thus, since \hat{f}_n is the ERM over $\mathcal{F}_{n, \alpha+\delta_n}^{\text{slide}}$, where $\delta_n > C_2 b_n > Mb'_n + C'_3 b_n + M_{\hat{f}_n} \tau_n$ for sufficiently large $C_2 > 0$ by assumption and $\mathbf{P}\{\mathcal{E}_n(C'_3 b_n + M_{\hat{f}_n} \tau_n)\} \geq 1 - 1/(4n)$, we have

$$\begin{aligned} \mathcal{E}(\hat{f}_n, f_n^*) & \leq L(\hat{f}_n) - L(f_n^*) - L_n(\hat{f}_n) + L_n(f_n^*) \\ & \leq 2\mathcal{R}(g(\mathcal{F})) + 4(\log 2 + 2F_0) \sqrt{\frac{2 \log(8n)}{n}} \end{aligned}$$

with probability at least $1 - 1/(2n)$, where we denote $L(f) = \mathbf{E}\{l(Y, f(X))\}$. Here, we let $g(f) := l(Y, f(\mathbf{X})) - l(Y, f_n^*(\mathbf{X}))$ and $g(\mathcal{F}) := \{g(f) : f \in \mathcal{F}\}$. The

second inequality follows from the Rademacher complexity bound in Lemma 2 with the fact that $|g(f)| \leq (\log 2 + 2F_0)$ for any $f \in \mathcal{F}$. Moreover, since $|g(f_1) - g(f_2)| \leq |f_1(\mathbf{X}) - f_2(\mathbf{X})|$ for any (\mathbf{X}, Y) due to the Lipschitz property of the logistic loss l , by Lemma 5, the preceding display is further bounded by

$$\frac{1}{\sqrt{n}} \sqrt{n^{\frac{d}{2\zeta+d}} (\log n)^3} = n^{-\frac{\zeta}{2\zeta+d}} (\log n)^{3/2} = b_n$$

up to some multiplicative constant. Therefore, there is a constant $C'_4 > 0$ such that

$$\begin{aligned} & \mathbf{P}\{\mathcal{E}(\hat{f}_n, f_\alpha^*) > C'_4 b_n + M_{\hat{f}_n} \tau_n\} \\ & \leq \mathbf{P}\{\mathcal{E}(\hat{f}_n, f_n^*) > (C'_4/2)b_n + M_{\hat{f}_n} \tau_n\} + \mathbf{P}\{\mathcal{E}(f_n^*, f_\alpha^*) > (C'_4/2)b_n + M_{\hat{f}_n} \tau_n\} \\ & \leq \mathbf{P}\{\{\mathcal{E}(\hat{f}_n, f_n^*) > (C'_4/2)b_n\} \cap \mathcal{E}_n(C'_3 b_n + M_{\hat{f}_n} \tau_n)\} + \mathbf{P}\{\mathcal{E}_n(C'_3 b_n + M_{\hat{f}_n} \tau_n)^c\} \\ & \quad + \mathbf{P}\{\|f_n^* - f_\alpha^*\|_\infty > (C'_4/2)b_n + M_{\hat{f}_n} \tau_n\} \\ & \leq 1 - n^{-1}, \end{aligned}$$

which completes the proof of the first assertion.

The second assertion follows from the fact that on $\mathcal{E}_n(C'_3 b_n + M_{\hat{f}_n} \tau_n)$,

$$\phi(\hat{f}_n) \leq \phi_{n, \tau_n}^{\text{slide}}(\hat{f}_n) + C'_3 b_n + M_{\hat{f}_n} \tau_n \leq \alpha + \delta_n + C'_3 b_n + M_{\hat{f}_n} \tau_n.$$

Case 2: UIF

The proof is almost the same as that of **Case 1**. The only difference is that we need to derive bounds of the Rademacher complexity $\widehat{\mathcal{R}}(\nu_{\tau_n} \circ \eta(\mathcal{F}))$ and the term $|\phi_{n, \tau_n}^{\text{slide}}(\hat{f}_n; \gamma, \epsilon) - \phi(\hat{f}_n; \gamma, \epsilon)|$. By Lemma 1,

$$|\nu_{\tau_n} \circ \eta_{f_1}(\mathbf{x}) - \nu_{\tau_n} \circ \eta_{f_2}(\mathbf{x})| \leq \frac{C'_1}{\tau_n} \|f_1 - f_2\|_\infty$$

for any f_1, f_2 and any \mathbf{x} for some $C'_1 > 0$. Therefore, we have that

$$\begin{aligned} \widehat{\mathcal{R}}(\nu_{\tau_n} \circ \eta(\mathcal{F})) & \leq \frac{4}{n} + \frac{12}{\sqrt{n}} \sqrt{S_n(L_n + 1) \log(n(L_n + 1)(N_n + 1)B_n/\tau_n))} \\ & \leq C'_2 n^{-\frac{\zeta}{2\zeta+d}} (\log n)^{3/2} = C'_2 b_n \end{aligned}$$

for some constant $C'_2 > 0$. In turn, similarly to the proof of **Case 1**, we have

$$\begin{aligned} \left| \phi_{n,\tau_n}^{\text{slide}}(\hat{f}_n; \gamma, \epsilon) - \phi(\hat{f}_n; \gamma, \epsilon) \right| &\leq 2\hat{\mathcal{R}}(\nu_{\tau_n} \circ \eta(\mathcal{F})) + 4\sqrt{\frac{2\log(4n)}{n}} + M_{\hat{f}_n} \tau_n \\ &\leq M_{\hat{f}_n} \tau_n + C'_4 b_n \end{aligned}$$

with probability $1 - 1/(4n)$ for some constant $C'_4 > 0$. Finally, we can complete the proof similarly to the proof of **Case 1**. \square

Proof of Proposition 1.

Proof. Note that $|\phi(f; \gamma, \epsilon) - \phi_{\tau_n}^{\text{slide}}(f; \gamma, \epsilon)| \leq |\phi_{\tau_n}^{\text{slide}}(f; \gamma, \epsilon) - \phi_{-\tau_n}^{\text{slide}}(f; \gamma, \epsilon)|$. By triangle inequality, we obtain

$$\begin{aligned} &|\phi_{\tau_n}^{\text{slide}}(f; \gamma, \epsilon) - \phi_{-\tau_n}^{\text{slide}}(f; \gamma, \epsilon)| \\ &\leq |\phi_{\tau_n}^{\text{slide}}(f; \gamma, \epsilon) - \phi_{n,\tau_n}^{\text{slide}}(f; \gamma, \epsilon)| + |\phi_{-\tau_n}^{\text{slide}}(f; \gamma, \epsilon) - \phi_{n,-\tau_n}^{\text{slide}}(f; \gamma, \epsilon)| \\ &\quad + |\phi_{n,\tau_n}^{\text{slide}}(f; \gamma, \epsilon) - \phi_{n,-\tau_n}^{\text{slide}}(f; \gamma, \epsilon)|. \end{aligned}$$

The first and second terms can be bounded as below using Lemmas 2 and 5 using the same arguments used in the proof of Theorem 3. That is, since the SLIDE functions ν_{τ_n} and $\nu_{-\tau_n}$ are $1/\tau_n$ -Lipschitz and bounded in $[0, 1]$, the first two terms are bounded by

$$\begin{aligned} &C' \left(\frac{1}{n} + \frac{1}{\sqrt{n}} \sqrt{S_n(L_n + 1) \log(n(L_n + 1)(N_n + 1)B_n/\tau_n))} \right) + 4\sqrt{\frac{2\log(1/(2\delta))}{n}} \\ &\leq C \left(\frac{1}{n} + \frac{1}{\sqrt{n}} \sqrt{n^{\frac{p}{2\zeta+p}} (\log n)^3} + \sqrt{\frac{\log(1/\delta)}{n}} \right) \end{aligned}$$

for some constant $C', C > 0$ with probability at least $1 - 2\delta$. Now let $b_n = n^{-\frac{\zeta}{2\zeta+p}(\log n)^{3/2}}$ up to constant with $\delta = 1/8n$ as is done in Theorem 3. Then we obtain that

$$|\phi_{\tau_n}^{\text{slide}}(f; \gamma, \epsilon) - \phi_{n,\tau_n}^{\text{slide}}(f; \gamma, \epsilon)| = \mathcal{O}(b_n)$$

and

$$|\phi_{-\tau_n}^{\text{slide}}(f; \gamma, \epsilon) - \phi_{n,-\tau_n}^{\text{slide}}(f; \gamma, \epsilon)| = \mathcal{O}(b_n).$$

Thus we conclude

$$|\phi_{\tau_n}^{\text{slide}}(f; \gamma, \epsilon) - \phi_{-\tau_n}^{\text{slide}}(f; \gamma, \epsilon)| \leq |\phi_{n, \tau_n}^{\text{slide}}(f; \gamma, \epsilon) - \phi_{n, -\tau_n}^{\text{slide}}(f; \gamma, \epsilon)| + \mathcal{O}(b_n)$$

and dividing by τ_n completes the proof. \square

Proof of Proposition 2.

Proof. By triangle inequality, $|\phi(f) - \phi_{\tau_n}^{\text{slide}}(f)| \leq |\phi_{\tau_n}^{\text{slide}}(f) - \phi_{n, \tau_n}^{\text{slide}}(f)| + |\phi(f) - \phi_n(f)| + |\phi_{n, \tau_n}^{\text{slide}}(f) - \phi_n(f)|$. The first term is bounded as below using Lemmas 2 and 5 by the same arguments used in the proof of Theorem 3. That is, since the SLIDE function ν_{τ_n} are $1/\tau_n$ -Lipschitz and bounded in $[0, 1]$, it is bounded by

$$\begin{aligned} & \sum_{z \in \{0,1\}} \left(\frac{8}{n_z} + \frac{24}{\sqrt{n_z}} \sqrt{S_n(L_n + 1) \log(n(L_n + 1)(N_n + 1)B_n)/\tau_n} + 4\sqrt{\frac{2 \log(4/\delta)}{n_z}} \right) \\ & \leq C \sum_{z \in \{0,1\}} \left(\frac{1}{n_z} + \frac{1}{\sqrt{n_z}} \sqrt{n^{\frac{p}{2\zeta+p}} (\log n)^3} + \sqrt{\frac{\log(1/\delta)}{n_z}} \right) \end{aligned}$$

for some constant $C > 0$ with probability at least $1 - 2\delta$. Now let $b_n = n^{-\frac{\zeta}{2\zeta+d}(\log n)^{3/2}}$ up to constant with $\delta = 1/8n$ as is done in Theorem 3. Then we obtain that $|\phi_{\tau_n}^{\text{slide}}(f) - \phi_{n, \tau_n}^{\text{slide}}(f)| = \mathcal{O}(b_n)$. On the other hand, using the inequality $||a - b| - |c - d|| \leq |a - c| + |b - d|$, the second term is bounded as

$$|\phi(f) - \phi_n(f)| = ||E^0 - E^1| - |E_n^0 - E_n^1|| \leq |E^0 - E_n^0| + |E^1 - E_n^1|$$

where $E^z = \mathbf{E}\{\mathbb{I}(f(\mathbf{X}) > 0)|Z = z\}$ and $E_n^z = \frac{1}{n_z} \sum_{z_i=z} \mathbb{I}(f(\mathbf{x}_i) > 0)$ for $z = 0, 1$. Note that $|E^z - E_n^z| = \max(E^z - E_n^z, E_n^z - E^z)$. Let $E_{\tau_n}^z = \mathbf{E}\{\nu_{\tau_n}(f(\mathbf{X}))|Z = z\}$ and $E_{n, \tau_n}^z = \frac{1}{n_z} \sum_{z_i=z} \nu_{\tau_n}(f(\mathbf{x}_i))$. Then,

$$E^z - E_n^z \leq E_{-\tau_n}^z - E_{n, \tau_n}^z \leq |E_{-\tau_n}^z - E_{n, -\tau_n}^z| + |E_{n, -\tau_n}^z - E_{n, \tau_n}^z| \leq C_1 b_n + |E_{n, -\tau_n}^z - E_{n, \tau_n}^z|$$

and

$$E_n^z - E^z \leq E_{n, -\tau_n}^z - E_{\tau_n}^z \leq |E_{n, -\tau_n}^z - E_{n, \tau_n}^z| + |E_{n, \tau_n}^z - E_{\tau_n}^z| \leq |E_{n, -\tau_n}^z - E_{n, \tau_n}^z| + C_2 b_n$$

for some constant $C_1, C_2 > 0$ by Lemmas 2 and 5 as is done in Theorem 3. Thus we have

$$\begin{aligned}
|\phi(f) - \phi_{\tau_n}^{\text{slide}}(f)| &\leq Cb_n + \sum_{z=0,1} |E_{n,-\tau_n}^z - E_{n,\tau_n}^z| + |\phi_{n,\tau_n}(f) - \phi_n(f)| \\
&= Cb_n + \sum_{z=0,1} \left| \frac{1}{n_z} \sum_{z_i=z} (\nu_{-\tau_n}(f(\mathbf{x}_i)) - \nu_{\tau_n}(f(\mathbf{x}_i))) \right| \\
&\quad + |\phi_{n,\tau_n}^{\text{slide}}(f) - \phi_n(f)|
\end{aligned}$$

for some $C > 0$. Dividing the above inequality by τ_n completes the proof. \square

D. Implementation details

We use a DNN model with one hidden layer of size 100 with the softmax function at the output layer. For the optimizers, the Adam [50] optimizer is used with scheduling the learning rates reducing by half at every 500 epochs. For the datasets, we describe the sample sizes and feature dimensions in Table D1. In addition, we introduce the actual hyperparameters used in learning in Table D1 with “Epochs” (the total number of iterations), “Optimizer” (the gradient descent optimization algorithm) and “lr” (the initial learning rate). We fix γ in UIF at 0.01 and choose $\tau \sim U(0.01, 0.2)$ along with random initials.

Table D1: Description of datasets and corresponding hyperparameters.

Dataset	<i>Adult</i>	<i>Bank</i>	<i>Law</i>
n (train / test)	36177 / 9044	32950 / 8238	21240 / 5310
d	41	47	11
Epochs	2000	2000	2000
Optimizer	Adam	Adam	Adam
lr	0.5	0.05	0.005
λ	(0.01, 10)	(0.01, 50)	(0.01, 100)
τ	$\sim U(0.01, 0.2)$	$\sim U(0.01, 0.2)$	$\sim U(0.01, 0.2)$
γ (UIF)	0.01	0.01	0.01

Evaluation measures. The balanced accuracy of a trained prediction model \hat{f} is $(\sum_{i:y_i=-1} \mathbb{I}(\hat{f}(\mathbf{x}_i) = y_i)/n_{-1} + \sum_{i:y_i=1} \mathbb{I}(\hat{f}(\mathbf{x}_i) = y_i)/n_1)/2$. For the consistency (Con.), we compute the rate of predictions that do not change when only the sensitive variable is changed. That is, Con. is computed as $\sum_{i=1}^n \mathbb{I}\{\hat{f}(\mathbf{x}_{i,z_i=0}) = \hat{f}(\mathbf{x}_{i,z_i=1})\}/n$, where $\mathbf{x}_{i,z_i=z}$ is an input vector which is the same as \mathbf{x}_i except $z_i = z$. Con. is initially considered by [44, 49]. The S-Con and GR-Con in Table 3 of Section 5 are the Con. values when z is the “spouse” variable and the multiples of “gender” and “race” variables, respectively.

Generating adversarial inputs for UIF. For UIF, in practice, we should compute an adversarial input $\mathbf{x}_{adv} := \arg \max_{\mathbf{x}' : d(\mathbf{x}, \mathbf{x}') \leq \epsilon} D(f(\mathbf{x}), f(\mathbf{x}'))$ of an arbitrary input \mathbf{x} . We use $\mathbf{x}_{adv} := \mathbf{x} + \mathbf{r}_{adv}$, where \mathbf{r}_{adv} is an adversarial direction. It is approximated by the second order Taylor’s polynomial with an approximated Hessian matrix as is proposed in VAT [56]. The source code that we use to generate \mathbf{x}_{adv} is a modified version of the source code from <https://github.com/lyakaap/VAT-pytorch/blob/master/vat.py>, where we replace the Kullback-Leibler divergence in VAT by the similarity metric D .

E. Additional experiments

We present the results of additional experiments.

An additional experiment similar to Figure 2. The 2-D dataset used in Figure 2 is generated from two Gaussians. We did a similar experiment with the two-moon dataset illustrated in the left panel of the Figure E1. Even though the datasets are completely different, the behaviors of the Hausdorff distances are similar in the sense that the hinge-surrogate fairness constraint does not approximate the original fairness constraint well while the SLIDE works well.

An example of inconsistency of fairness for the hinge-surrogate fairness constraint. Let $X \in \mathbb{R}$ be a random variable having the distribution as $X|Z = z \sim \mathcal{N}(z, 1)$ for $z \in \{-1, 1\}$. For \mathcal{F} , we consider linear models as $\mathcal{F} = \beta_0 + \beta x : \beta_0 \in [-1, 1], \beta \in [-1, 1]$. Note that $\beta_0 + \beta X|Z = z \sim \mathcal{N}(\beta_0 + \beta z, \beta^2)$. Hence, the DI

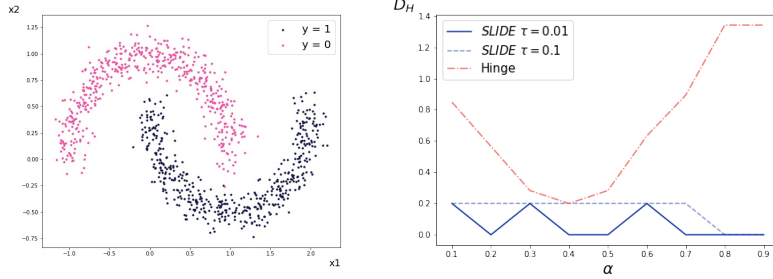


Figure E1: (Left) The two-moon dataset. (Right) Plot of α vs. d_α^{hinge} and $d_{\alpha,\tau}^{\text{slide}}$ for $\tau \in \{0.01, 0.1\}$.

value for given (β_0, β) is computed by $\text{DI}(\beta_0, \beta) = |\Phi(-\beta_0/\beta + 1) - \Phi(-\beta_0/\beta - 1)|$, where $\Phi(\cdot)$ is the cumulative distribution of $\mathcal{N}(0, 1)$. On the other hand, by formula of the mean of the truncated normal distribution, we have $\mathbf{E}\{(\beta_0 + \beta \mathbf{X} + 1)_+ | Z = z\} = \beta_0 + \beta z + 1 + \frac{\phi(-(\beta_0 + \beta z + 1)/\beta)}{1 - \Phi(-(\beta_0 + \beta z + 1)/\beta)}$ where $\phi(\cdot)$ is the probability density function of $\mathcal{N}(0, 1)$. Thus we have

$$\text{DI}^{\text{hinge}}(\beta_0, \beta) = \left| -2\beta + \frac{\phi(-(\beta_0 - \beta + 1)/\beta)}{1 - \Phi(-(\beta_0 - \beta + 1)/\beta)} - \frac{\phi(-(\beta_0 + \beta + 1)/\beta)}{1 - \Phi(-(\beta_0 + \beta + 1)/\beta)} \right|.$$

The left panel of Figure E2 draws the d_α^{hinge} from $\text{DI}^{\text{hinge}}(\beta_0, \beta)$ above, which clearly shows that the hinge-surrogate fairness constraint is not consistent in fairness.

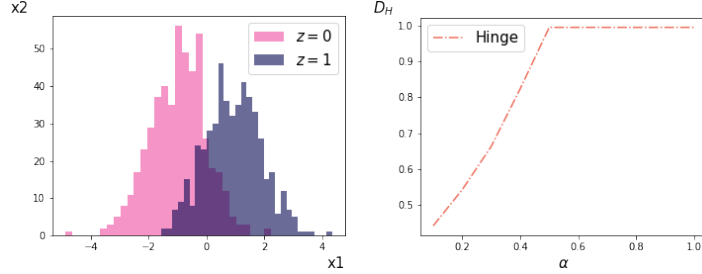


Figure E2: (Left) The generated dataset, $X|Z = z \sim \mathcal{N}(z, 1)$. (Right) Plot of α vs. d_α^{hinge} .

Application of CCCP to UIF + SLIDE. We can apply the CCCP algorithm [45] to find a local solution to the UIF + SLIDE constrained empirical risk minimization problem. The advantage of the CCCP algorithm is that it always

converges to a local minimum. Note that the SLIDE function ν_τ can be decomposed to the sum of the convex function $\nu_{\text{conv}}(z) = (z)_+/\tau$ and the concave function $\nu_{\text{conc}} = -(z - \tau)_+/\tau$. Note that we are to find a (local) minimum of $L_n(f) + \lambda\phi_{n,\tau}^{\text{slide}}(f; \gamma, \epsilon)$. Let f^{curr} be the current solution. Then, the CCCP algorithm updates f by minimizing

$$L_n(f) + \lambda \left\{ \phi_{n,\tau}^{\text{slide, conv}}(f; \gamma, \epsilon) + f^\top \nabla \phi_{n,\tau}^{\text{slide, conc}}(f^{\text{curr}}; \gamma, \epsilon) \right\},$$

where

$$\phi_{n,\tau}^{\text{slide, conv}}(f; \gamma, \epsilon) = \frac{1}{n} \sum_{i=1}^n \{D(f(\mathbf{x}_i), f(\mathbf{v}_i)) - \gamma\}_+ / \tau$$

and

$$\phi_{n,\tau}^{\text{slide, conc}}(f; \gamma, \epsilon) = -\frac{1}{n} \sum_{i=1}^n \{D(f(\mathbf{x}_i), f(\mathbf{v}_i)) - \gamma - \tau\}_+ / \tau,$$

and \mathbf{v}_i is the adversarial input of \mathbf{x}_i , that is, $\mathbf{v}_i = \arg \max_{\mathbf{v}; d(\mathbf{x}_i, \mathbf{v}) \leq \epsilon} D(f(\mathbf{x}_i), f(\mathbf{v}))$.

Tables E1 and E2 are the reproductions of Tables 2 and 3 in the main manuscript with adding the results of the CCCP algorithm. The results suggest that the CCCP algorithm with the SLIDE is a promising alternative to the standard gradient descent algorithm.

Table E1: Comparison of UIF + { Hinge, SLIDE, HySLIDE, SLIDE (CCCP) } on *Adult*, *Bank* and *Law* test datasets.

Dataset	UIF	+ Hinge	+ SLIDE	+ HySLIDE	+ SLIDE (CCCP)
<i>Adult</i>	Acc	84.60	84.36	84.51	84.52
	BA	75.75	75.73	75.69	75.70
	Con. (se)	.918 (.003)	.920 (.005)	.922 (.003)	.921 (.004)
<i>Bank</i>	Acc	90.29	90.14	90.15	90.73
	BA	63.82	63.43	63.03	63.11
	Con. (se)	.985 (.006)	.990 (.005)	.984 (.004)	.985 (.007)
<i>Law</i>	Acc	83.75	83.99	84.02	84.11
	BA	62.67	62.71	62.79	62.66
	Con. (se)	.985 (.006)	.986 (.004)	.987 (.003)	.992 (.006)

Table E2: Performances (Acc(%), BA(%), S-Con., and GR-Con.) of individually fair prediction models including one learned with the CCCP algorithm on *Adult* test dataset. For SenSeI [44] and SenSR [49], we copied the results from [44].

<i>Adult</i>	Acc	BA	S-Con.	GR-Con.
UIF + Hinge	85.3	76.8	.936	.967
UIF + SLIDE	85.1	76.6	.970	.985
UIF + HySLIDE	85.2	76.6	.976	.981
UIF + SLIDE (CCCP)	85.2	76.8	<u>.974</u>	.968
SenSeI [44]	-	76.8	.945	.963
SenSR [49]	78.7	78.9	.934	<u>.984</u>

References

- [1] J. Angwin, J. Larson, S. Mattu, L. Kirchner, Machine bias, ProPublica, May 23 (2016) 2016.
- [2] J. Kleinberg, J. Ludwig, S. Mullainathan, A. Rambachan, Algorithmic fairness, in: Aea papers and proceedings, Vol. 108, 2018, pp. 22–27.
- [3] N. Mehrabi, F. Morstatter, N. Saxena, K. Lerman, A. Galstyan, A survey on bias and fairness in machine learning, arXiv preprint arXiv:1908.09635.
- [4] T. Calders, F. Kamiran, M. Pechenizkiy, Building classifiers with independence constraints, in: 2009 IEEE International Conference on Data Mining Workshops, IEEE, 2009, pp. 13–18.
- [5] S. Barocas, A. D. Selbst, Big data’s disparate impact, California Law Review 104 (3) (2016) 671–732.
URL <http://www.jstor.org/stable/24758720>
- [6] M. Hardt, E. Price, N. Srebro, Equality of opportunity in supervised learning, in: Advances in neural information processing systems, 2016, pp. 3315–3323.

[7] C. Dwork, M. Hardt, T. Pitassi, O. Reingold, R. Zemel, Fairness through awareness, in: Proceedings of the 3rd Innovations in Theoretical Computer Science Conference, ITCS '12, Association for Computing Machinery, New York, NY, USA, 2012, p. 214–226. doi:10.1145/2090236.2090255.
 URL <https://doi.org/10.1145/2090236.2090255>

[8] F. Kamiran, T. Calders, Data preprocessing techniques for classification without discrimination, *Knowledge and Information Systems* 33 (1) (2012) 1–33.

[9] R. Zemel, Y. Wu, K. Swersky, T. Pitassi, C. Dwork, Learning fair representations, in: International Conference on Machine Learning, 2013, pp. 325–333.

[10] M. Feldman, S. A. Friedler, J. Moeller, C. Scheidegger, S. Venkatasubramanian, Certifying and removing disparate impact, in: proceedings of the 21th ACM SIGKDD international conference on knowledge discovery and data mining, 2015, pp. 259–268.

[11] F. Calmon, D. Wei, B. Vinzamuri, K. N. Ramamurthy, K. R. Varshney, Optimized pre-processing for discrimination prevention, in: Advances in Neural Information Processing Systems, 2017, pp. 3992–4001.

[12] L. Dixon, J. Li, J. Sorensen, N. Thain, L. Wasserman, Measuring and mitigating unintended bias in text classification, in: Proceedings of the 2018 AAAI/ACM Conference on AI, Ethics, and Society, 2018, pp. 67–73.

[13] K. Webster, M. Recasens, V. Axelrod, J. Baldridge, Mind the gap: A balanced corpus of gendered ambiguous pronouns, *Transactions of the Association for Computational Linguistics* 6 (2018) 605–617.

[14] D. Xu, S. Yuan, L. Zhang, X. Wu, Fairgan: Fairness-aware generative adversarial networks, in: 2018 IEEE International Conference on Big Data (Big Data), IEEE, 2018, pp. 570–575.

- [15] E. Creager, D. Madras, J.-H. Jacobsen, M. Weis, K. Swersky, T. Pitassi, R. Zemel, Flexibly fair representation learning by disentanglement, in: International Conference on Machine Learning, PMLR, 2019, pp. 1436–1445.
- [16] N. Quadrianto, V. Sharmanska, O. Thomas, Discovering fair representations in the data domain, in: Proceedings of the IEEE/CVF Conference on Computer Vision and Pattern Recognition, 2019, pp. 8227–8236.
- [17] T. Kamishima, S. Akaho, H. Asoh, J. Sakuma, Fairness-aware classifier with prejudice remover regularizer, in: Joint European Conference on Machine Learning and Knowledge Discovery in Databases, Springer, 2012, pp. 35–50.
- [18] G. Goh, A. Cotter, M. Gupta, M. P. Friedlander, Satisfying real-world goals with dataset constraints, in: Advances in Neural Information Processing Systems, 2016, pp. 2415–2423.
- [19] Y. Bechavod, K. Ligett, Learning fair classifiers: A regularization-inspired approach, arXiv preprint arXiv:1707.00044 (2017) 1733–1782.
- [20] M. B. Zafar, I. Valera, M. G. Rogriguez, K. P. Gummadi, Fairness constraints: Mechanisms for fair classification, in: Artificial Intelligence and Statistics, 2017, pp. 962–970.
- [21] A. Agarwal, A. Beygelzimer, M. Dudik, J. Langford, H. Wallach, A reductions approach to fair classification, in: J. Dy, A. Krause (Eds.), Proceedings of the 35th International Conference on Machine Learning, Vol. 80 of Proceedings of Machine Learning Research, PMLR, 2018, pp. 60–69.
URL <https://proceedings.mlr.press/v80/agarwall18a.html>
- [22] A. K. Menon, R. C. Williamson, The cost of fairness in binary classification, in: Conference on Fairness, Accountability and Transparency, 2018, pp. 107–118.

- [23] H. Narasimhan, Learning with complex loss functions and constraints, in: International Conference on Artificial Intelligence and Statistics, PMLR, 2018, pp. 1646–1654.
- [24] A. Cotter, H. Jiang, K. Sridharan, Two-player games for efficient non-convex constrained optimization, in: ALT, 2019.
- [25] L. E. Celis, L. Huang, V. Keswani, N. K. Vishnoi, Classification with fairness constraints: A meta-algorithm with provable guarantees, in: Proceedings of the Conference on Fairness, Accountability, and Transparency, 2019, pp. 319–328.
- [26] M. B. Zafar, I. Valera, M. Gomez-Rodriguez, K. P. Gummadi, Fairness Constraints: A Flexible Approach for Fair Classification., *J. Mach. Learn. Res.* 20 (75) (2019) 1–42.
- [27] J. Cho, C. Suh, G. Hwang, A fair classifier using kernel density estimation, in: 34th Conference on Neural Information Processing Systems, NeurIPS 2020, Conference on Neural Information Processing Systems, 2020.
- [28] R. Vogel, A. Bellet, S. Clémenton, Learning Fair Scoring Functions: Fairness Definitions, Algorithms and Generalization Bounds for Bipartite Ranking, arXiv preprint arXiv:2002.08159.
- [29] F. Kamiran, A. Karim, X. Zhang, Decision theory for discrimination-aware classification, in: 2012 IEEE 12th International Conference on Data Mining, IEEE, 2012, pp. 924–929.
- [30] B. Fish, J. Kun, Á. D. Lelkes, A confidence-based approach for balancing fairness and accuracy, in: Proceedings of the 2016 SIAM International Conference on Data Mining, SIAM, 2016, pp. 144–152.
- [31] S. Corbett-Davies, E. Pierson, A. Feller, S. Goel, A. Huq, Algorithmic decision making and the cost of fairness, in: Proceedings of the 23rd ACM SIGKDD International Conference on Knowledge Discovery and Data Mining, 2017, pp. 797–806.

[32] G. Pleiss, M. Raghavan, F. Wu, J. Kleinberg, K. Q. Weinberger, On fairness and calibration, in: Advances in Neural Information Processing Systems, 2017, pp. 5680–5689.

[33] E. Chzhen, C. Denis, M. Hebiri, L. Oneto, M. Pontil, Leveraging labeled and unlabeled data for consistent fair binary classification, in: Advances in Neural Information Processing Systems, 2019, pp. 12760–12770.

[34] R. Jiang, A. Pacchiano, T. Stepleton, H. Jiang, S. Chiappa, Wasserstein fair classification, in: Uncertainty in Artificial Intelligence, PMLR, 2020, pp. 862–872.

[35] D. Wei, K. N. Ramamurthy, F. Calmon, Optimized score transformation for fair classification, Vol. 108 of Proceedings of Machine Learning Research, PMLR, Online, 2020, pp. 1673–1683.
 URL <http://proceedings.mlr.press/v108/wei20a.html>

[36] T. Zhang, Statistical behavior and consistency of classification methods based on convex risk minimization, *The Annals of Statistics* 32 (1) (2004) 56–85.

[37] P. L. Bartlett, M. I. Jordan, J. D. McAuliffe, Convexity, classification, and risk bounds, *Journal of the American Statistical Association* 101 (473) (2006) 138–156.

[38] G. Blanchard, O. Bousquet, P. Massart, Statistical performance of support vector machines, *The Annals of Statistics* 36 (2) (2008) 489–531.

[39] B. Woodworth, S. Gunasekar, M. I. Ohannessian, N. Srebro, Learning non-discriminatory predictors, in: S. Kale, O. Shamir (Eds.), *Proceedings of the 2017 Conference on Learning Theory*, Vol. 65 of *Proceedings of Machine Learning Research*, PMLR, 2017, pp. 1920–1953.
 URL <http://proceedings.mlr.press/v65/woodworth17a.html>

[40] M. Donini, L. Oneto, S. Ben-David, J. S. Shawe-Taylor, M. Pontil, Empirical risk minimization under fairness constraints, in: Advances in Neural Information Processing Systems, 2018, pp. 2791–2801.

[41] Y. Wu, L. Zhang, X. Wu, On convexity and bounds of fairness-aware classification, in: The World Wide Web Conference, WWW '19, Association for Computing Machinery, New York, NY, USA, 2019, p. 3356–3362. doi:10.1145/3308558.3313723.
URL <https://doi.org/10.1145/3308558.3313723>

[42] M. Lohaus, M. Perrot, U. V. Luxburg, Too relaxed to be fair, in: H. D. III, A. Singh (Eds.), Proceedings of the 37th International Conference on Machine Learning, Vol. 119 of Proceedings of Machine Learning Research, PMLR, 2020, pp. 6360–6369.
URL <https://proceedings.mlr.press/v119/lohaus20a.html>

[43] G. Yona, G. Rothblum, Probably approximately metric-fair learning, in: J. Dy, A. Krause (Eds.), Proceedings of the 35th International Conference on Machine Learning, Vol. 80 of Proceedings of Machine Learning Research, PMLR, Stockholmsmässan, Stockholm Sweden, 2018, pp. 5680–5688.

[44] M. Yurochkin, Y. Sun, Sensei: Sensitive set invariance for enforcing individual fairness (2020). arXiv:2006.14168.

[45] A. L. Yuille, A. Rangarajan, The concave-convex procedure (cccp), in: T. Dietterich, S. Becker, Z. Ghahramani (Eds.), Advances in Neural Information Processing Systems, Vol. 14, MIT Press, 2002, pp. 1033–1040.

[46] X. Shen, G. C. Tseng, X. Zhang, W. H. Wong, On ψ -learning, Journal of the American Statistical Association 98 (463) (2003) 724–734.

[47] D. Dua, C. Graff, UCI machine learning repository (2017).
URL <http://archive.ics.uci.edu/ml>

[48] M. Lichman, UCI machine learning repository (2013).
 URL <http://archive.ics.uci.edu/ml>

[49] D. Mukherjee, M. Yurochkin, M. Banerjee, Y. Sun, Two simple ways to learn individual fairness metrics from data, in: Proceedings of the 37th International Conference on Machine Learning, 2020, pp. 7097–7107.

[50] D. P. Kingma, J. Ba, Adam: A method for stochastic optimization, in: Y. Bengio, Y. LeCun (Eds.), 3rd International Conference on Learning Representations, ICLR 2015, San Diego, CA, USA, May 7-9, 2015, Conference Track Proceedings, 2015.
 URL <http://arxiv.org/abs/1412.6980>

[51] S. Shalev-Shwartz, S. Ben-David, Understanding machine learning: From theory to algorithms, Cambridge university press, 2014.

[52] M. M. Wolf, Mathematical foundations of supervised learning (2018).

[53] T. Suzuki, Adaptivity of deep reLU network for learning in besov and mixed smooth besov spaces: optimal rate and curse of dimensionality, in: International Conference on Learning Representations, 2019.
 URL <https://openreview.net/forum?id=H1ebTsActm>

[54] S. A. van de Geer, Empirical processes in m-estimation, 2000.

[55] J. Schmidt-Hieber, et al., Nonparametric regression using deep neural networks with relu activation function, Annals of Statistics 48 (4) (2020) 1875–1897.

[56] T. Miyato, S. ichi Maeda, M. Koyama, S. Ishii, Virtual adversarial training: A regularization method for supervised and semi-supervised learning (2018). arXiv:1704.03976.